



CMS-HIN-14-016



CERN-PH-EP/2015-329

2022/03/23

Correlations between jets and charged particles in PbPb and pp collisions at $\sqrt{s_{\text{NN}}} = 2.76 \text{ TeV}$

The CMS Collaboration^{*}

Abstract

The quark-gluon plasma is studied via medium-induced changes to correlations between jets and charged particles in PbPb collisions compared to pp reference data. This analysis uses data sets from PbPb and pp collisions with integrated luminosities of $166 \mu\text{b}^{-1}$ and 5.3 pb^{-1} , respectively, collected at $\sqrt{s_{\text{NN}}} = 2.76 \text{ TeV}$. The angular distributions of charged particles are studied as a function of relative pseudorapidity ($\Delta\eta$) and relative azimuthal angle ($\Delta\phi$) with respect to reconstructed jet directions. Charged particles are correlated with all jets with transverse momentum (p_{T}) above 120 GeV , and with the leading and subleading jets (the highest and second-highest in p_{T} , respectively) in a selection of back-to-back dijet events. Modifications in PbPb data relative to pp reference data are characterized as a function of PbPb collision centrality and charged particle p_{T} . A centrality-dependent excess of low- p_{T} particles is present for all jets studied, and is most pronounced in the most central events. This excess of low- p_{T} particles follows a Gaussian-like distribution around the jet axis, and extends to large relative angles of $\Delta\eta \approx 1$ and $\Delta\phi \approx 1$.

Submitted to the Journal of High Energy Physics

1 Introduction

The quark-gluon plasma (QGP) produced in ultra-relativistic heavy ion collisions may be probed *in situ* via partons produced in the initial hard-scatterings, which carry high transverse momentum (p_T) compared to most of the particles in the event. In the QGP, partons are expected to suffer energy loss in the medium, a phenomenon known as “jet quenching” [1]. This effect was discovered at RHIC via observables including suppression of high- p_T particle production [2] and charged particle correlations [3]. Jet quenching has been studied at the CERN LHC via high- p_T particle suppression [4–6], and via the momentum balance of reconstructed back-to-back dijets. In these latter studies, dijet transverse momentum balance was investigated in PbPb, pPb and in pp collisions [7–10]. Significant imbalance was found in central PbPb collisions, consistent with a pathlength-dependent energy loss in the QGP medium. In peripheral PbPb collisions and in pPb collisions, the dijet momentum balance is comparable to the one measured in pp collisions, thus confirming that the energy loss in central PbPb collisions is not due to initial state cold nuclear matter effects. In the QGP, the interaction of the hard-scattered partons (and their fragmentation products) with the medium leads to a redistribution of energy carried by the produced particles. Comparing the charged-particle distributions from heavy ion data to the pp reference can help to differentiate between energy loss models and ultimately constrain the properties of the QGP [11–14].

Early RHIC studies of two-particle correlations involving a leading high- p_T (8–15 GeV) particle did not find a significant modification in the distribution of the associated particles at small angles from the leading particle. A quenching effect was found in the distribution of particles opposite in azimuth to the leading particle, observed as a reduction in the associated yield [15–19]. These results could be interpreted as an in-medium energy loss (in which associated particles fully thermalize and do not retain correlation to the jet direction) followed by a vacuum-like fragmentation of the remaining jet [20]. Compared to the capabilities of the LHC, these studies at RHIC are significantly limited by the lower production rates for hard probes. Subsequent high-precision measurements at the LHC [21–23] have shown that the detailed jet structures within a jet cone radius of 0.3 are modified by the medium in terms of both p_T and angular distributions. However, these observed in-cone changes only explain a small fraction of the dijet momentum imbalance, indicating that a large amount of energy is radiated outside of the jet cone or transferred to particles with very low momentum. Direct measurements of energy redistribution between event hemispheres containing subleading and leading jets were made by CMS via the “missing- p_T ” observable [10, 24]. These studies found the overall energy flow to be modified in PbPb collisions out to large radial distances from the dijet axis, and various theoretical models have since attempted to describe the result [25–27]. Extending measurements of jet structure modifications to similarly large angles is crucial to properly constrain the energy loss mechanism.

In this paper, we use $166 \mu b^{-1}$ of PbPb collisions taken during the 2011 LHC heavy ion run at a nucleon-nucleon center-of-mass energy of $\sqrt{s_{NN}} = 2.76$ TeV. For the reference measurement, we use pp data taken in 2013 at the same center-of-mass energy corresponding to an integrated luminosity of 5.3 pb^{-1} . Two-dimensional angular correlations were previously studied in CMS for pairs of charged particles [28]. In the present analysis, this technique is applied to correlate jets with charged particles. For each charged particle and reconstructed jet, p_T and pseudorapidity (η) are measured with respect to the beam axis, and azimuthal angle (ϕ) is measured in the transverse plane. From these measurements, the relative pseudorapidity ($\Delta\eta = \eta_{\text{track}} - \eta_{\text{jet}}$) and relative azimuth ($\Delta\phi = \phi_{\text{track}} - \phi_{\text{jet}}$) between jets and charged-particle tracks is determined. These relative angles are used to construct two-dimensional $\Delta\eta$ – $\Delta\phi$ charged particle density distributions, which we will refer to as “jet-track correlations”. The jet-track correla-

tions are then studied as a function of centrality (defined as a percentile of the total inelastic cross section, with 0% indicating collisions with impact parameter $b = 0$) and charged-particle transverse momentum (p_T^{trk}).

In order to extend these measurements to low p_T^{trk} , where soft particles resulting from energy loss mechanisms such as gluon radiation are expected to appear, an analysis must carefully handle both large combinatorial backgrounds typical for the heavy ion environment, and long-range correlations arising from hydrodynamic expansion [29]. Taking advantage of the kinematic reach of hard probes and the availability of detailed characterization of the event bulk properties, the CMS detector permits the statistical separation of the medium-related modifications of jet-track correlations from the long-range hydrodynamic background. Using this technique, this study captures jet-related energy flow both inside and outside of the jet cone, extending measurements of intrinsic jet properties to large relative angles in $\Delta\eta$ and $\Delta\phi$.

2 The CMS detector

The central feature of the CMS apparatus is a superconducting solenoid with an internal diameter of 6 m, providing an axial uniform magnetic field of 3.8 T. Muons are measured in gas-ionization detectors embedded in the steel flux-return yoke outside the solenoid. Within the solenoid volume are a silicon pixel and strip tracker, a lead tungstate crystal electromagnetic calorimeter (ECAL), and a brass and scintillator hadron calorimeter (HCAL), each composed of a barrel and two endcap sections. Extensive hadronic forward (HF) steel and quartz fiber calorimetry complements the barrel and endcap detectors, providing coverage to $|\eta| < 5$. In this analysis, the collision centrality is determined using the total sum of transverse energy (E_T) from calorimeter towers in the HF region (covering $2.9 < |\eta| < 5.2$). For the forward region $2.9 < |\eta| < 5.0$ relevant for collision centrality determination, HF fibers are bundled in towers with widths of 0.175×0.175 ($\Delta\eta \times \Delta\phi$) [30]. The distribution (E_T) is used to divide the event sample into bins, each representing 0.5% of the total nucleus-nucleus hadronic interaction cross section. A detailed description of centrality determination can be found in Ref. [8].

Jet reconstruction for this analysis relies on calorimeter information from the ECAL and HCAL. For the central region $|\eta| < 1.6$ in which jets are selected for this analysis, the HCAL cells have widths of 0.087 in both η and ϕ . In the η - ϕ plane, and for $|\eta| < 1.48$, the HCAL cells map on to 5×5 ECAL crystals arrays to form calorimeter towers projecting radially outwards from close to the nominal interaction point. The barrel section of the ECAL has an energy resolution of 1%–2.5%, while the endcaps have an energy resolution of 2.5–4% [31]. Within each tower, the energy deposits in ECAL and HCAL cells are summed to define the calorimeter tower energies, subsequently used to provide the energies and directions of hadronic jets. When combining information from the entire detector, the jet energy resolution amounts typically to 15% at 10 GeV, 8% at 100 GeV, and 4% at 1 TeV, to be compared to about 40%, 12%, and 5% obtained when the ECAL and HCAL calorimeters alone are used [30].

Accurate particle tracking is critical for measurements of charged-hadron yields. The CMS silicon tracker measures charged particles within the region $|\eta| < 2.5$. For particles of $1 < p_T < 10$ GeV and $|\eta| < 1.4$, the track resolutions are typically 1.5% in p_T and 25–90 (45–150) μm in the transverse (longitudinal) impact parameter with respect to the collision vertex [32]. A detailed description of the CMS detector, together with a definition of the coordinate system used and the relevant kinematic variables, can be found in Ref. [33].

3 Jet and track reconstruction and corrections

For both pp and PbPb collisions, jet reconstruction is performed with the anti- k_T algorithm, encoded in the FASTJET framework [34, 35]. Following previous CMS studies [10, 21–23], a narrow jet reconstruction distance parameter, $R = 0.3$, is chosen due to the large underlying event in heavy ion collisions. Jet p_T and direction in η and ϕ are determined based on iterative clustering of energy deposits in the CMS calorimeters. For PbPb collisions, the CMS algorithm “HF/Voronoi” is used to subtract the heavy ion underlying event [36]. This algorithm estimates the underlying event contribution to the E_T in each calorimeter tower by performing a singular value decomposition of the particle distributions. The average E_T , as a function of η and ϕ , is subtracted from each calorimeter tower, and then the energy is redistributed between neighboring calorimeter towers so that no tower contains non-physical negative E_T . For pp collisions no underlying event subtraction is employed, as the effect of the underlying event on the jet energy is small relative to the jet energy scale (JES) uncertainty.

Monte Carlo (MC) event generators have been used for evaluation of the jet and track reconstruction performance, in particular for determining the tracking efficiency as well as the jet energy response and resolution. Jet events are generated with PYTHIA [37] (version 6.423, tune Z2 [38]). These generated PYTHIA events are propagated through the CMS detector using the GEANT4 package [39] to simulate the detector response. In order to account for the influence of the underlying PbPb events, the PYTHIA events are embedded into fully simulated PbPb events that are generated by HYDJET [40] (version 1.8), which is tuned to reproduce the total particle multiplicities, charged-hadron spectra, and elliptic flow at all centralities. The embedding is performed by mixing the simulated digital signal information from PYTHIA and HYDJET, hereafter referred to as PYTHIA+HYDJET. No simulation of jet quenching is applied in this PYTHIA+HYDJET simulation. These events are then propagated through the same reconstruction and analysis procedures used for data events. The JES is established using PYTHIA and PYTHIA+HYDJET events in bins of event centrality as a function of p_T , η , and number of charged particles inside the jet cone. For studies of pp data and PYTHIA simulation, charged particles are reconstructed using the same iterative method [32] as in the previous CMS analyses of pp collisions. For PbPb data and PYTHIA+HYDJET MC, an iterative charged-particle reconstruction similar to that of earlier heavy ion analyses [5, 22] is employed, as described in detail in Ref. [24].

4 Data samples and triggers

The first level (L1) of the CMS trigger system, composed of custom hardware processors, uses information from the calorimeters and muon detectors to select the most interesting events in a fixed time interval of less than 4 μs . The high-level trigger (HLT) processor farm further decreases the event rate from around 100 kHz to less than 1 kHz before data storage. The events for this analysis were selected using an HLT that selects all events containing at least one calorimeter jet with $p_T > 80 \text{ GeV}$. The HLT is fully efficient for events containing offline reconstructed jets with $p_T > 120 \text{ GeV}$. In order to suppress noise due to noncollision sources such as cosmic rays and beam backgrounds, the events used in this analysis were further required to satisfy offline selection criteria as documented in Refs. [8, 41]. These criteria include selecting only events with a reconstructed vertex including at least two tracks and a z position within 15 cm of the detector center, and requiring energy deposits in at least 3 forward calorimeter towers on either side of the interaction point.

The offline selection of events begins with jets reconstructed as described in Section 3. To study

the jet-track correlations, the events are then categorized into two samples: an inclusive selection of high- p_T jets and a selection of back-to-back dijet events. For the inclusive sample, jets are required to have $p_T > 120\text{ GeV}$ and to fall within $|\eta| < 1.6$, with multiple jets from the same event permitted in this inclusive jet sample. These inclusive selection criteria match previous CMS studies [22, 23] that measured jet fragmentation functions and jet shapes within the jet cone ($\Delta R < 0.3$), and allow this analysis to extend comparable measurements to large angles from the jet axis. We then separately select a dijet sample using criteria matched to those of a previous analysis that explores dijet energy balance [10]. In this dijet selection, events are first required to contain a highest p_T (leading) calorimeter jet in the range of $|\eta| < 2$, with a corrected jet $p_T > 120\text{ GeV}$ and a next-highest p_T (subleading) jet of $p_T > 50\text{ GeV}$, also in $|\eta| < 2$. The azimuthal angle between the leading and subleading jets is required to be at least $5\pi/6$. No explicit requirement is made either on the presence or absence of a third jet in the event. To ensure stable jet reconstruction performance, only events in which both leading and subleading jets fall within $|\eta| < 1.6$ are included in the final data sample.

5 Jet-track angular correlations

Charged tracks in the event with p_T^{trk} above 1 GeV are used to construct two-dimensional $\Delta\eta$ - $\Delta\phi$ correlations with respect to the individually measured jet axis for inclusive jets and for leading and subleading jets in dijet events. The jet-track correlations are constructed according to the procedure established in Ref. [42], for the following bins in p_T^{trk} : 1–2, 2–3, 3–4, and 4–8 GeV. This work does not attempt to construct correlations below 1 GeV , where the jet-related signal is very small compared to the combinatorial and long-range correlated background, or for $p_T^{\text{trk}} > 8\text{ GeV}$ where the statistical power becomes limited. The correlations are corrected for tracking efficiency and misreconstruction on a per-track basis, using an efficiency parametrization defined as a function of centrality, p_T^{trk} , η , ϕ , and radial distance from the nearest jet with $p_T > 50\text{ GeV}$ [24].

Correlations are formed by measuring angular distances to the inclusive, leading and subleading jet axes for each p_T^{trk} range. The signal pair distribution, $S(\Delta\eta, \Delta\phi)$, represents the per-track efficiency-corrected yield of jet-track pairs N^{same} from the same event normalized by the total number of jets:

$$S(\Delta\eta, \Delta\phi) = \frac{1}{N_{\text{jets}}} \frac{d^2 N^{\text{same}}}{d\Delta\eta d\Delta\phi}. \quad (1)$$

To correct for pair acceptance effects, we use the mixed event technique [28, 43, 44] to determine the geometrical $\Delta\eta$ - $\Delta\phi$ shape that arises from selecting jets and tracks from within our respective acceptances of $|\eta_{\text{jet}}| < 1.6$ and $|\eta_{\text{track}}| < 2.4$. In this technique, a mixed event distribution, $ME(\Delta\eta, \Delta\phi)$, is constructed by correlating the reconstructed jet axis direction from a selected signal event to tracks from events in a minimum bias data sample. For each signal event, 40 minimum bias events are selected to have a similar vertex position (within 1 cm) and event centrality (within 2.5%) to the jet event. Mixed event correlations are corrected for tracking efficiency and misreconstruction on a per-track basis applying the same efficiency parametrization used to correct signal correlations. The distribution of such mixed event jet-track pairs N^{mix} is denoted:

$$ME(\Delta\eta, \Delta\phi) = \frac{1}{N_{\text{jets}}} \frac{d^2 N^{\text{mix}}}{d\Delta\eta d\Delta\phi}. \quad (2)$$

This distribution $ME(\Delta\eta, \Delta\phi)$ is normalized to unity at $(\Delta\eta = 0, \Delta\phi = 0)$, where jets and tracks are close together and therefore have full pair acceptance. Correlations are corrected for

pair acceptance effects by dividing them by the normalized mixed event distribution $ME(\Delta\eta, \Delta\phi)/ME(0,0)$. The resulting yield of associated tracks per jet is defined as:

$$\frac{1}{N_{\text{jets}}} \frac{d^2N}{d\Delta\eta d\Delta\phi} = ME(0,0) \frac{S(\Delta\eta, \Delta\phi)}{ME(\Delta\eta, \Delta\phi)}. \quad (3)$$

This process is illustrated in Fig. 1: the raw correlations to the leading and subleading jets in dijet events are shown on the left for the lowest p_T^{trk} bin (1–2 GeV) and 0–10% centrality range. The jet-like peak at $(\Delta\eta, \Delta\phi) = (0,0)$ is visible about both the leading and the subleading jets despite the high background levels in these most central events. An away-side peak at $(\Delta\eta, \Delta\phi) = (0, \pi)$ is also visible in both leading and subleading jet correlations, corresponding in the leading jet correlation to the $\Delta\eta$ -smeared subleading jet peak, and likewise corresponding to the $\Delta\eta$ -smeared leading jet peak in the subleading jet correlation. The middle panel shows the shape of the pair acceptance correction determined using the mixed event technique. Finally, on the right, we present the acceptance-corrected correlations for the same p_T^{trk} bin before the subtraction of long-range correlation terms.

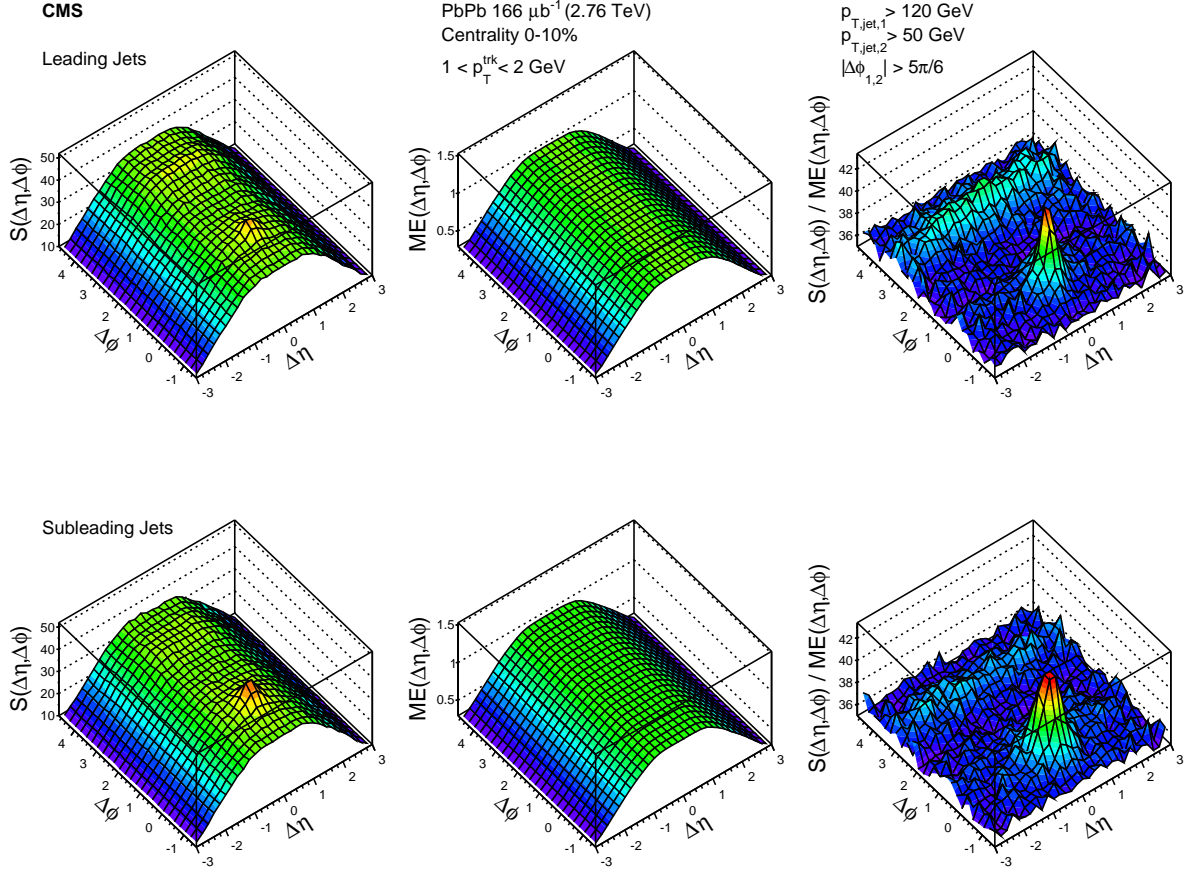


Figure 1: Jet-track correlation signal shape $S(\Delta\eta, \Delta\phi)$ for tracks with $1 < p_T^{\text{trk}} < 2$ GeV in 0–10% central events (left), and corresponding mixed event shape $ME(\Delta\eta, \Delta\phi)$ for the same centrality and p_T^{trk} bin (center). Their ratio gives the acceptance-corrected yield (right). The top row shows the correlation between leading jets (with $p_{T,\text{jet},1} > 120$ GeV) and all tracks, while the bottom row shows the correlation between subleading jets (with $p_{T,\text{jet},2} > 50$ GeV) and all tracks.

To subtract the random combinatorial backgrounds and long-range correlations (dominated by hydrodynamic flow in PbPb and momentum conservation constraints in pp events), we

employ a sideband subtraction technique in which these backgrounds are approximated by the measured two-dimensional correlations in the range $1.5 < |\Delta\eta| < 3.0$. Based on a CMS study that shows no appreciable variation of the elliptic flow for charged particles with $p_T^{\text{trk}} > 1 \text{ GeV}$ in the $\Delta\eta$ interval of ± 3.0 relevant for the present analysis [45], the Fourier harmonics are assumed to be constant in $\Delta\eta$. This background distribution in relative azimuthal angle (integrated over $1.5 < |\Delta\eta| < 3.0$) is then fitted with a function modeling harmonic flow plus a term to capture the (Gaussian or sharper) peak at $\Delta\phi = \pi$ associated with the (smeared) jet opposite to the jet under study:

$$B(\Delta\phi) = B_0(1 + 2V_1 \cos(\Delta\phi) + 2V_2 \cos(2\Delta\phi) + 2V_3 \cos(3\Delta\phi)) + A_{\text{AS}} \exp\left[-\left(\frac{|\Delta\phi - \pi|}{\alpha}\right)^{\beta}\right], \quad (4)$$

where B_0 is the overall background level; V_1 , V_2 , and V_3 are Fourier coefficients modeling harmonic flow; and A_{AS} , α , and β are respectively the magnitude, width, and shape parameters of the away-side peak. We find that at low p_T^{trk} the long-range azimuthal sideband distributions are exhausted by the first three Fourier coefficients (V_1 , V_2 , V_3), while at high p_T^{trk} , V_1 and V_2 are sufficient to describe the background level within statistical uncertainties. Figure 2 illustrates the background subtraction process. The long-range contributions of the full 2D correlation (left) are estimated by the $\Delta\phi$ projection (shown in the middle panel) of this correlation over the range $1.5 < |\Delta\eta| < 3.0$. The fit to this $\Delta\phi$ distribution is propagated uniformly in $\Delta\eta$, and subtracted from the acceptance-corrected yield. The short-range correlations remaining after this background subtraction are shown on the right panel, again for $p_T^{\text{trk}} = 1\text{--}2 \text{ GeV}$.

Jet-track correlations obtained from PbPb data are compared with those obtained from the pp reference data. To ensure that the kinematic range of the jets included in this comparison is the same, correlations are reweighted on a jet-by-jet basis so that the resulting jet p_T spectrum matches that of PbPb data for a given centrality class. Weighting factors are derived from the ratio of the normalized PbPb to pp jet spectra in bins of 10 GeV . The reference pp jet p_T spectrum is also smeared to account for jet energy resolution differences between the PbPb and pp samples. Reference correlations in $\Delta\eta$ and $\Delta\phi$ are then constructed and analyzed following the procedure described above for PbPb data.

6 Corrections and systematic uncertainties

An analysis of PYTHIA and PYTHIA+HYDJET MC simulated events is performed to evaluate and correct for the effects of two jet reconstruction biases on the measured correlated yield: a bias toward the selection of jets with harder fragmentation, and a bias toward the selection of jets that coincide with upward fluctuations in the background. The first correction addresses a jet fragmentation function (JFF) bias in which the jet energy is over-estimated for jets with hard fragmentation and under-estimated for those with soft fragmentation, resulting in a preferred selection of jets with harder fragmentation. This bias affects pp and PbPb data similarly, and results in a reduction in the charged-particle correlated yield. To correct for this effect in pp data, we compare correlations between reconstructed versus generated jets and generated particles in PYTHIA simulations, and subtract the difference (reconstructed minus generated) from data correlations. For the corresponding PbPb correction, we consider PYTHIA jets embedded into and reconstructed within a HYDJET-simulated environment, comparing correlations between generated versus reconstructed jets and the generated particles corresponding to the embedded PYTHIA hard-scattering. We note that this procedure also corrects for jet axis smearing in

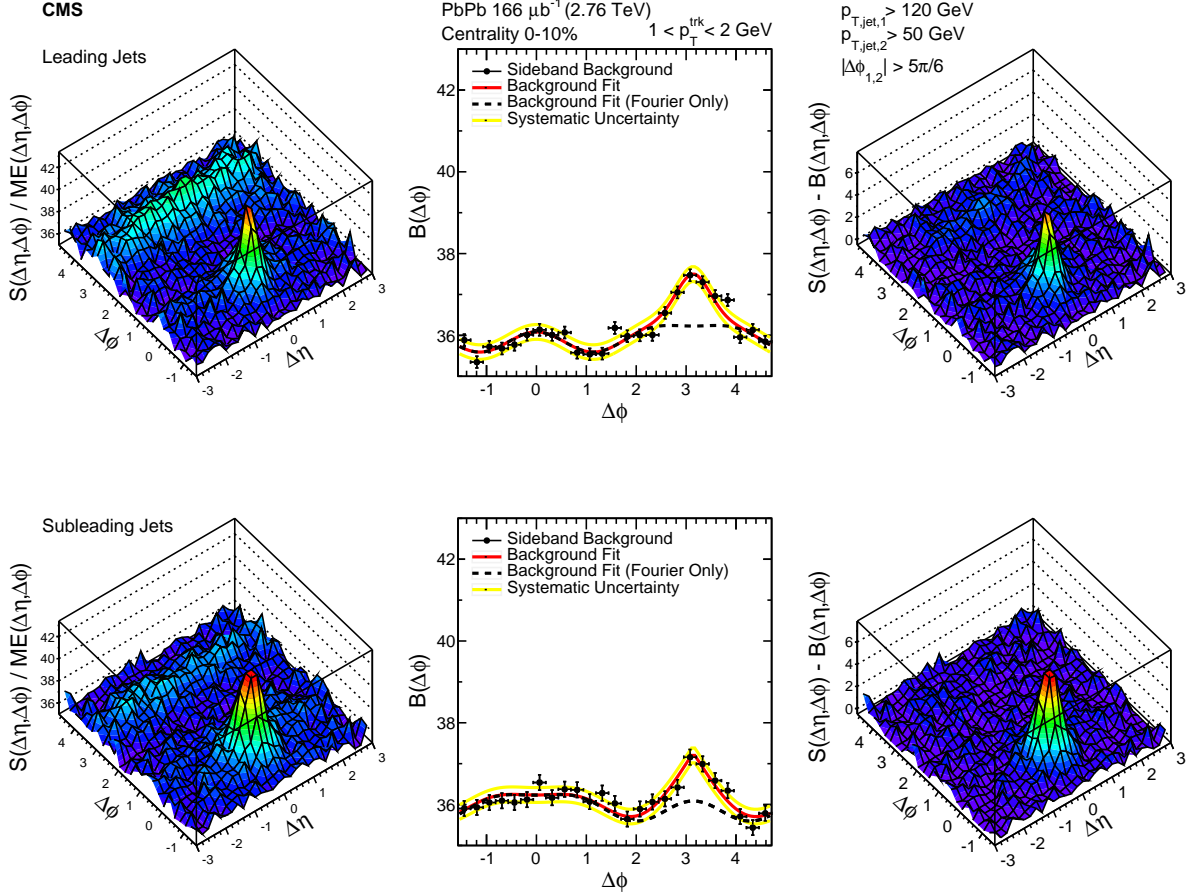


Figure 2: Acceptance-corrected 2D jet-track correlation yield (left) is projected over the range $1.5 < |\Delta\eta| < 3.0$, producing a 1D background distribution (center). The fit to this distribution (indicated with a red dark line) is subtracted from the total yield to obtain the 2D background-subtracted yield shown on the right (for tracks with $1 < p_T^{\text{trk}} < 2 \text{ GeV}$). The black dashed line shows the background level and Fourier flow harmonic components of the fit only, excluding the away-side peak. Yellow lines in the $B(\Delta\phi)$ plot (middle panel) indicate the systematic uncertainty assigned to the background subtraction.

reconstruction, which is found to have no significant effect on the total integral of the correlation, and to affect the correlation shapes only within $\Delta\eta < 0.2$ and $\Delta\phi < 0.2$. The magnitude of this correction (relative to the total correlated yield) ranges from 3 to 6% in pp data, and from 3 to 7% in PbPb data. In PYTHIA+HYDJET, this JFF bias correction is found to be centrality-independent (and very similar to that for PYTHIA), and is applied as a single correction for all centrality bins. Maximum variations between centrality bins are used to evaluate the systematic uncertainty in this correction, which is found to be within 2% of the correlated yield at low p_T^{trk} and decreasing to zero at high p_T^{trk} .

The second correction evaluates and subtracts the measured charged-particle yield resulting from the preferential selection of jets that coincide with upward fluctuations in the background as detailed in Ref. [23]. The selections of inclusive and leading jets with $p_T > 120 \text{ GeV}$ and sub-leading jets with $p_T > 50 \text{ GeV}$ are sensitive to fluctuations in the background. Lower-energy jets that coincide with upward fluctuations in the background are included in the sample, while higher-energy jets that coincide with downward background fluctuations are excluded. Because the inclusive and leading jet p_T spectra are both steeply falling, the inclusion in the sam-

ple of a jet coinciding with an upward fluctuation in the background is much more common than the exclusion of a jet coinciding with a downward fluctuation, resulting in an excess of background tracks near the jet axis. To quantify this effect, we performed the full analysis using a sample of PYTHIA jets embedded into a HYDJET heavy ion environment, and then extracted the correlated yield (with respect to reconstructed jets) comprised of particles originating from the HYDJET background. This correction was also checked with a data-driven technique using minimum bias PbPb events to confirm that HYDJET appropriately reproduces fluctuations in the PbPb background, and the resulting upward bias in charged-particle correlated yields when these fluctuations contribute to the reconstructed jet energy. This background fluctuation bias strongly depends on event centrality and p_T^{trk} , with a magnitude of up to 24% of the corrected signal for the lowest p_T tracks in the most central collisions, decreasing to within 3% for high- p_T tracks and to a negligible contribution in peripheral collisions. This correlated yield due to the background fluctuation bias is subtracted to correct PbPb data, and half its magnitude is applied as a systematic uncertainty.

In addition to the systematic uncertainty associated with these two jet-reconstruction-related corrections, other sources of systematic uncertainty in this analysis include the JES determination, track reconstruction, and the procedures applied to correct for pair acceptance effects and subtract the uncorrelated and long-range backgrounds. The correlated yield uncertainty associated with the JES is assessed by varying the inclusive and leading jet p_T selection threshold up and down by 3% (according to the JES uncertainty and also including differences in quark versus gluon JES [24]). The resulting maximum variations in total correlated particle yield are found to be within 3% in all cases, and we assign a 3% systematic uncertainty to account for this effect. The uncertainties of the p_T -dependent tracking efficiency and misidentified track corrections are found to be within 3–4% in PbPb and pp collisions, and are independent of the centrality of the collisions. To account for the possible track reconstruction differences in data and simulation, a residual 5% uncertainty is applied based on observed variations in corrected to initial track p_T and η spectra for different track quality selections [24].

We evaluate pair acceptance uncertainties by considering differences in the background levels measured separately in each of the two sideband regions of our acceptance-corrected correlations ($-3.0 < \Delta\eta < -1.5$ and $1.5 < \Delta\eta < 3.0$). This results in an uncertainty within the range of 5–9%. The overall systematic uncertainty due to background subtraction is calculated by varying all fit parameters up and down by their respective uncertainties and calculating the maximum resulting differences in background level, and by considering the deviation from the “0” level after background subtraction in the sideband region $1.5 < |\Delta\eta| < 3.0$. In more central events (0–10%), the background subtraction uncertainty is found to be within 2–5% for the lowest p_T^{trk} bin where the background is most significant compared to the signal level.

All systematic uncertainties, evaluated as a function of p_T^{trk} and event centrality are summarized in Table 1 as fractions of the total measured yield. The range of uncertainties listed presents the variation with track transverse momentum, with larger uncertainty values corresponding to the lowest p_T^{trk} bin (1–2 GeV) for all sources. The systematic uncertainties from all seven sources are added in quadrature to obtain the total systematic uncertainty, which is quoted as a fraction of the total charged-particle yield associated with the jet under study.

7 Results

In this analysis, jet-track correlations are studied differentially in centrality and p_T^{trk} . Correlations are projected in $\Delta\eta$ and $\Delta\phi$ to probe possible differences between azimuthal and pseudo-rapidity distributions. Figures 3 and 4 show inclusive jet correlations projected on the $\Delta\eta$ (over

Table 1: Systematic uncertainties in the measurement of the jet-track correlations in PbPb and pp collisions, as percentage of the total measured correlated yield. The numbers presented in this table summarize the range of values of systematic uncertainty (as a function of p_T^{trk}) for different centrality bins.

Source	0–10%	10–30%	30–50%	50–100%	pp
Background fluctuation bias	3–12%	2–7%	1–5%	0–1%	—
Jet fragmentation function bias	0–2%	0–2%	0–2%	0–2%	0–2%
Residual jet energy scale	3%	3%	3%	3%	3%
Tracking efficiency uncertainty	4%	4%	4%	4%	3%
Residual track efficiency corr.	5%	5%	5%	5%	5%
Pair acceptance corrections	5–9%	5–9%	4–8%	2–6%	2–3%
Background subtraction	2–5%	2–5%	2–5%	2–5%	1–2%
Total	9–17%	9–14%	8–13%	8–10%	7–8%

$|\Delta\phi| < 1.0$) and $\Delta\phi$ (over $|\Delta\eta| < 1.0$) axes respectively for the lowest p_T^{trk} selection. The upper panels of each figure present the centrality evolution of the correlations for inclusive jets with $p_T > 120 \text{ GeV}$, together with a reference measurement from pp data at the same collision energy shown with open symbols. To better visualize the PbPb to pp comparisons, the difference of the PbPb and pp correlation distributions is presented in the bottom panel for all centralities. Correlations are symmetrized in $\Delta\eta$ and $\Delta\phi$ for clarity.

For the most peripheral events studied (centrality 50–100%), the PbPb correlations at low transverse momentum, $1 < p_T^{\text{trk}} < 2 \text{ GeV}$, show a very small excess (at most slightly larger than the uncertainties) relative to the pp reference data. This excess grows with collision centrality, with the most significant excess present in the most central collisions. The shape of this excess in the low- p_T^{trk} per-jet particle yields is found to be similar in the $\Delta\eta$ and $\Delta\phi$ distributions, and in both dimensions exhibits a Gaussian-like shape that extends to large relative angles $\Delta\eta \approx 1$ and $\Delta\phi \approx 1$. We note that these results are consistent with previous CMS studies of jet-shape modifications [22] and fragmentation functions [23] within the previously studied small $\Delta R < 0.3$ region, while extending measurements to individually study $\Delta\eta$ and $\Delta\phi$ distributions over the full range $\Delta\eta$ and $\Delta\phi < 1.5$.

The next two figures present the results of the jet-track correlation measurements for dijets with leading jet $p_T > 120 \text{ GeV}$ and subleading jet $p_T > 50 \text{ GeV}$, obeying the back-to-back angular selection criteria previously described. Figure 5 presents the projection of jet-track correlations measured for charged tracks with p_T^{trk} between 1 and 2 GeV on the $\Delta\eta$ axis for the leading (upper panel) and subleading (middle panel) jets, while Fig. 6 shows the corresponding projections on the $\Delta\phi$ axis. Again pp data are included for comparison, and for the most peripheral (50–100% central) PbPb events the correlations are similar to the pp reference for the leading jets, and differ only slightly for the subleading jets. As in the case of inclusive jets, differences of correlations between pp and PbPb collisions gradually increase from peripheral to central collisions, and are most pronounced in the 0–10% central events for both leading and subleading jets. We note that there is little difference between the leading and inclusive jet correlated-yield distributions, indicating that the requirement that leading jets have the highest p_T in the event does not significantly bias the selection of jets with $p_T > 120 \text{ GeV}$.

For this lowest p_T^{trk} bin shown, we observe that (as for the inclusive jet selection) the excess of correlated yield extends significantly beyond the typical jet reconstruction radius for both leading and subleading jets. The soft excess is more pronounced on the more “quenched” subleading side, but is also present on the leading side. This indicates that leading jets, although surface-biased toward shorter path-lengths through the medium, also experience quenching in

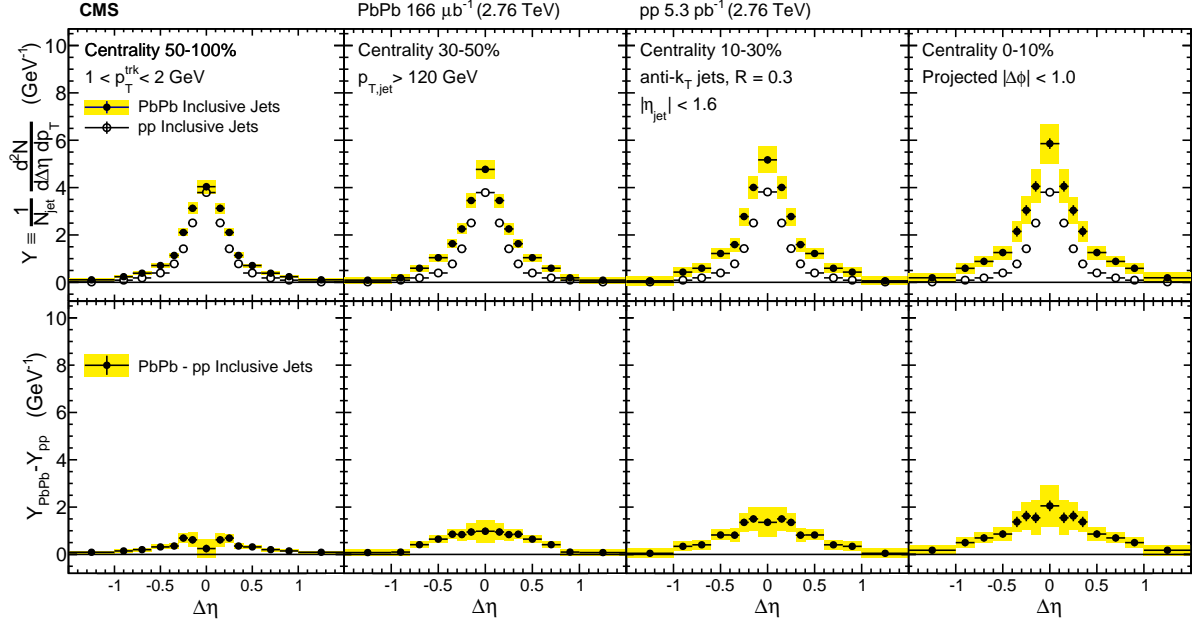


Figure 3: Symmetrized $\Delta\eta$ distributions (projected over $|\Delta\phi| < 1$) of background-subtracted particle yields correlated to PbPb and pp inclusive jets with $p_T > 120$ GeV are shown in the top panels for tracks with $1 < p_T^{\text{trk}} < 2$ GeV. The difference in PbPb and pp per-jet yields is shown in the bottom panels. The total systematic uncertainties are shown as shaded boxes, and statistical uncertainties are shown as vertical bars (often smaller than the symbol size).

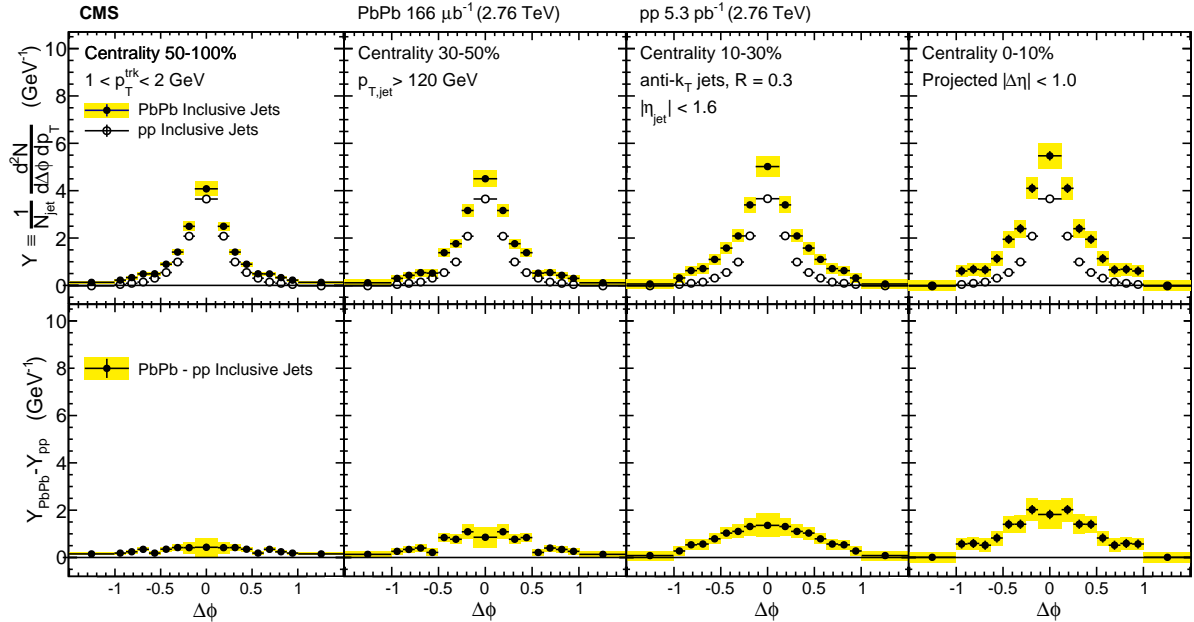


Figure 4: Symmetrized $\Delta\phi$ distributions (projected over $|\Delta\eta| < 1$) of background-subtracted particle yields correlated to PbPb and pp inclusive jets with $p_T > 120$ GeV are shown in the top panels for tracks with $1 < p_T^{\text{trk}} < 2$ GeV. The difference in PbPb and pp per-jet yields is shown in the bottom panels. The total systematic uncertainties are shown as shaded boxes, and statistical uncertainties are shown as vertical bars (often smaller than the symbol size).

central PbPb collisions. To better illustrate both subleading and leading modifications, the last row of Figs. 5 and 6 shows the differences (PbPb minus pp) of the correlations in the two upper

panels.

To quantify the total per-jet excess yield observed in the PbPb data with respect to the pp reference, we plot the integrals of the excess yields (PbPb minus pp) as a function of p_T^{trk} and collision centrality in Fig. 7. As the figure shows, in both leading and subleading jets, the excess yield diminishes for higher momentum tracks until the yield becomes similar to the pp reference for the highest p_T^{trk} bin of 4–8 GeV. As seen in previous figures, central collisions exhibit the largest low- p_T^{trk} excesses. This demonstrates the expected trend corresponding to quenching of both the leading and the subleading jets, as energy from particles with higher p_T^{trk} is redistributed into particles with lower p_T^{trk} via interactions with the medium.

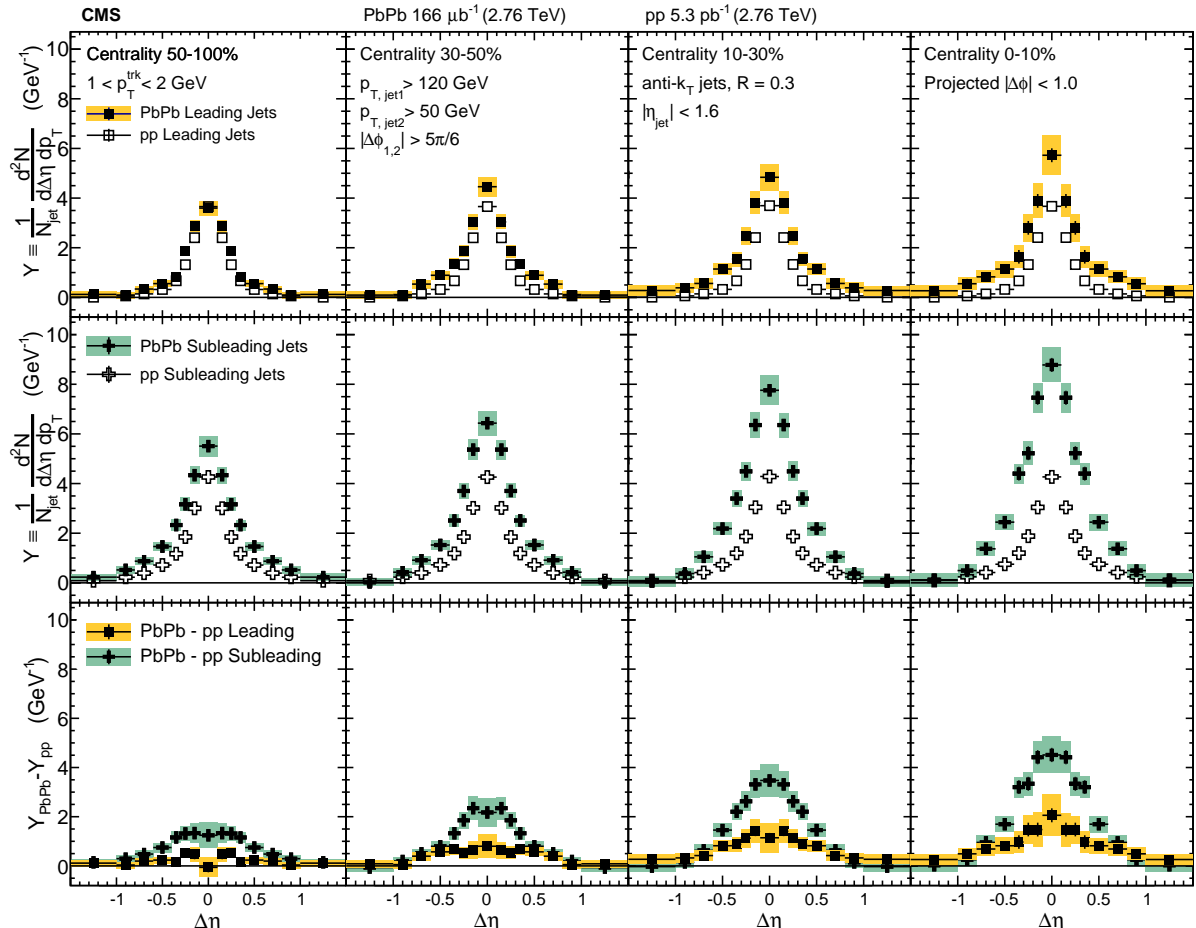


Figure 5: The top panels show the $\Delta\eta$ distributions (projected over $|\Delta\phi| < 1$) of charged-particle background-subtracted yields correlated to PbPb and pp leading jets with $p_{T,\text{jet}1} > 120 \text{ GeV}$. The middle panels show the same distributions for subleading jets with $p_{T,\text{jet}2} > 50 \text{ GeV}$, and the bottom panels show the difference PbPb minus pp for both leading and subleading jets. The total systematic uncertainties are shown as shaded boxes, and statistical uncertainties are shown as vertical bars (often smaller than the symbol size).

In order to characterize the angular widths of the charged-particle distributions in $\Delta\eta$ and $\Delta\phi$, we fit the measured correlations with a double Gaussian function (which was found to best describe the overall correlation shapes). The width is defined as the region around zero in $|\Delta\eta|$ or $|\Delta\phi|$ that contains 67% of the total correlated yield. Width uncertainties are calculated by repeating the measurement for the $\Delta\eta$ and $\Delta\phi$ distributions varied by their respective systematic uncertainties, which are treated as fully correlated for the purposes of this determination.

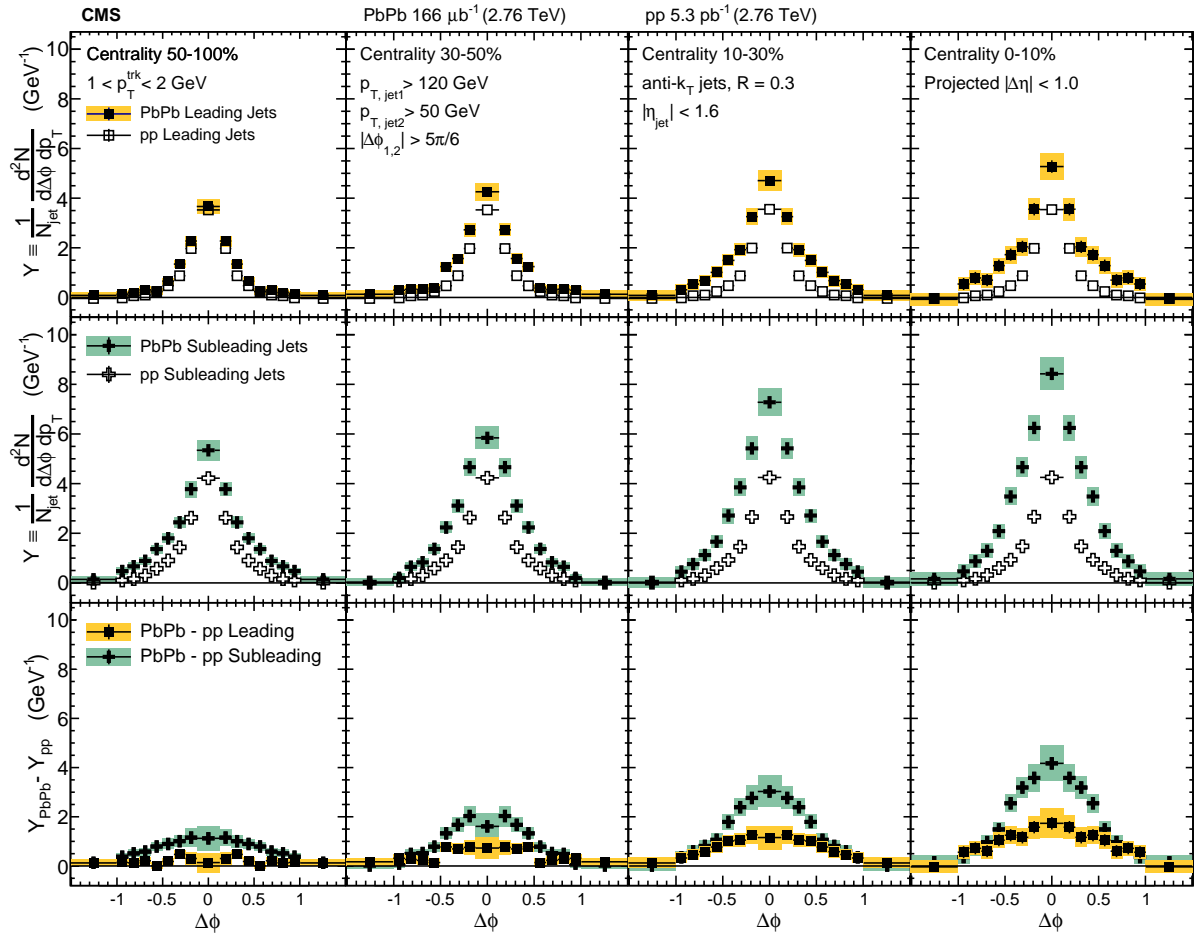


Figure 6: The top panels show the $\Delta\phi$ distributions (projected over $|\Delta\eta| < 1$) of charged-particle background-subtracted yields correlated to PbPb and pp leading jets with $p_{T,\text{jet}1} > 120 \text{ GeV}$. The middle panels show the same distributions for subleading jets with $p_{T,\text{jet}2} > 50 \text{ GeV}$, and the bottom panels show the difference PbPb minus pp for both leading and subleading jets. The total systematic uncertainties are shown as shaded boxes, and statistical uncertainties are shown as vertical bars (often smaller than the symbol size).

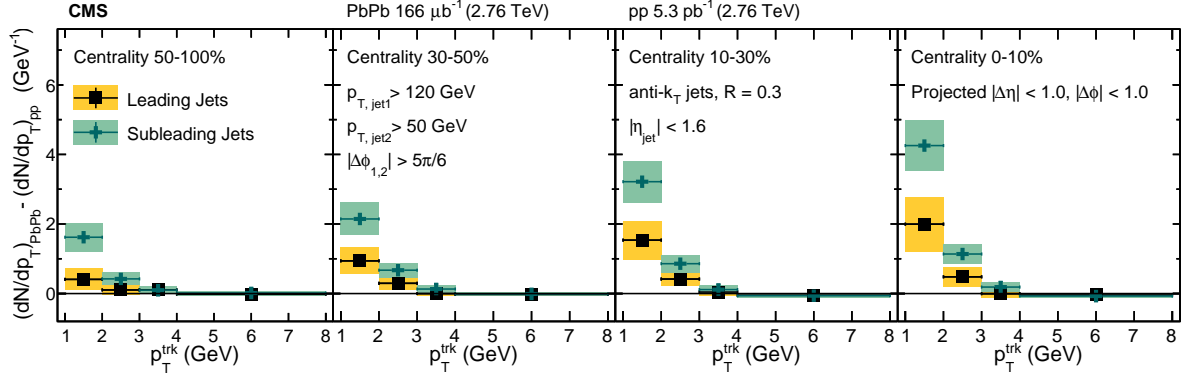


Figure 7: Total excess correlated yield observed in the PbPb data with respect to the reference measured in pp collisions, shown as a function of track p_T in four different centrality intervals (0–10%, 10–30%, 30–50%, 50–100%) for both leading jets with $p_{T,jet1} > 120 \text{ GeV}$ and subleading jets with $p_{T,jet2} > 50 \text{ GeV}$. The total systematic uncertainties are shown as shaded boxes, and statistical uncertainties are shown as vertical bars (often smaller than the symbol size).

Widths for leading and subleading jet correlations in $\Delta\eta$ and $\Delta\phi$ are presented as a function of p_T^{trk} in Figs. 8–11. Distributions of low- p_T tracks correlated with either of the two jets are found to be significantly broader in central PbPb events compared to those in pp data in both $\Delta\eta$ and $\Delta\phi$ dimensions. This broadening is greatest for the low- p_T tracks and in the most central events, and diminishes quickly with increasing track momenta. Above 4 GeV, the widths measured in PbPb and pp events are the same within the systematic uncertainties. We note that the width of the PbPb minus pp excess yield is similar for leading and subleading jets. In pp data, however, the peak associated with the subleading jet is softer and broader than the peak associated with the leading jet. There is therefore a larger difference in peak width when comparing PbPb leading jet peaks to the narrow pp leading jet peaks (Figs. 8–9), and a smaller difference when comparing PbPb subleading jet peaks to the broader pp subleading jet peaks (Figs. 10–11).

8 Summary

In this analysis, jet-track correlations have been studied as a function of $\Delta\eta$ and $\Delta\phi$ with respect to the jet axis in PbPb and pp collisions at $\sqrt{s_{\text{NN}}} = 2.76 \text{ TeV}$. Two-dimensional angular correlations have been considered for charged particles with $p_T^{\text{trk}} > 1 \text{ GeV}$ as a function of p_T^{trk} and collision centrality for two jet selections. A sample of inclusive jets above the jet momentum threshold of 120 GeV was studied, as well as a sample of dijet events selected to include a leading jet with $p_T > 120 \text{ GeV}$ and a subleading jet with $p_T > 50 \text{ GeV}$. In all cases, an excess of soft particle yields was observed in central PbPb collisions with respect to pp reference data, similar for inclusive and leading jet samples and larger for the (more-quenched) subleading jet sample. The low- p_T^{trk} (1–3 GeV) excess-yield distributions were studied individually and, in both $\Delta\eta$ and $\Delta\phi$, they exhibit similar Gaussian-like distributions out to large relative angles ($\Delta\eta \approx 1$ and $\Delta\phi \approx 1$) from the jet axis. The excess was found to be largest at the lowest p_T^{trk} (1–2 GeV) in the most central (0–10%) PbPb data, and to decrease gradually with centrality. For peripheral (50–100%) PbPb collisions, correlated low- p_T^{trk} particle yields are only slightly larger than those for the pp reference. The excess also gradually decreases with increasing p_T^{trk} until yields of particles with $p_T^{\text{trk}} > 4 \text{ GeV}$ are similar to pp reference data, consistent with the results of a previous CMS jet quenching study. This new correlation analysis provides a comprehensive evaluation of medium effects on jet properties, extending information about jet shapes to

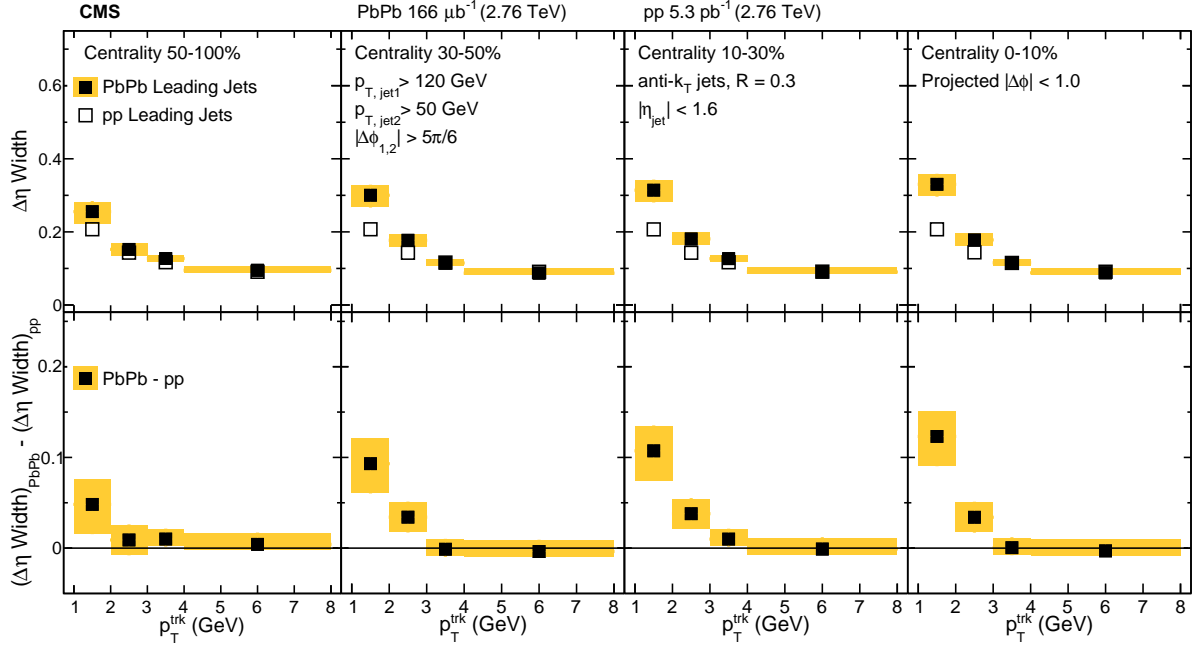


Figure 8: Comparison of the widths in PbPb and pp of the $\Delta\eta$ charged-particle distributions correlated to leading jets with $p_{T,\text{jet}1} > 120 \text{ GeV}$, as a function of p_T^{trk} . The bottom row shows the difference of the widths in PbPb and pp data. The shaded band corresponds to systematic uncertainty, and statistical uncertainties are smaller than symbol size.

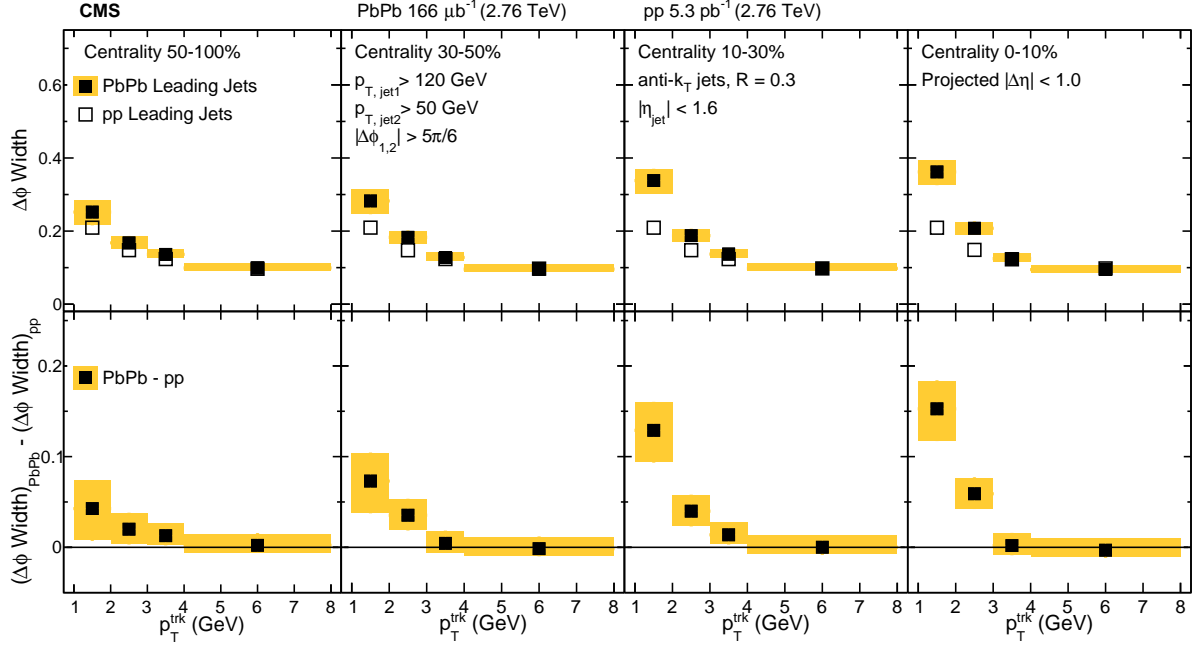


Figure 9: Comparison of the widths in PbPb and pp of the $\Delta\phi$ charged-particle distributions correlated to leading jets with $p_{T,\text{jet}1} > 120 \text{ GeV}$, as a function of p_T^{trk} . The bottom row shows the difference of the widths in PbPb and pp data. The shaded band corresponds to systematic uncertainty, and statistical uncertainties are smaller than symbol size.

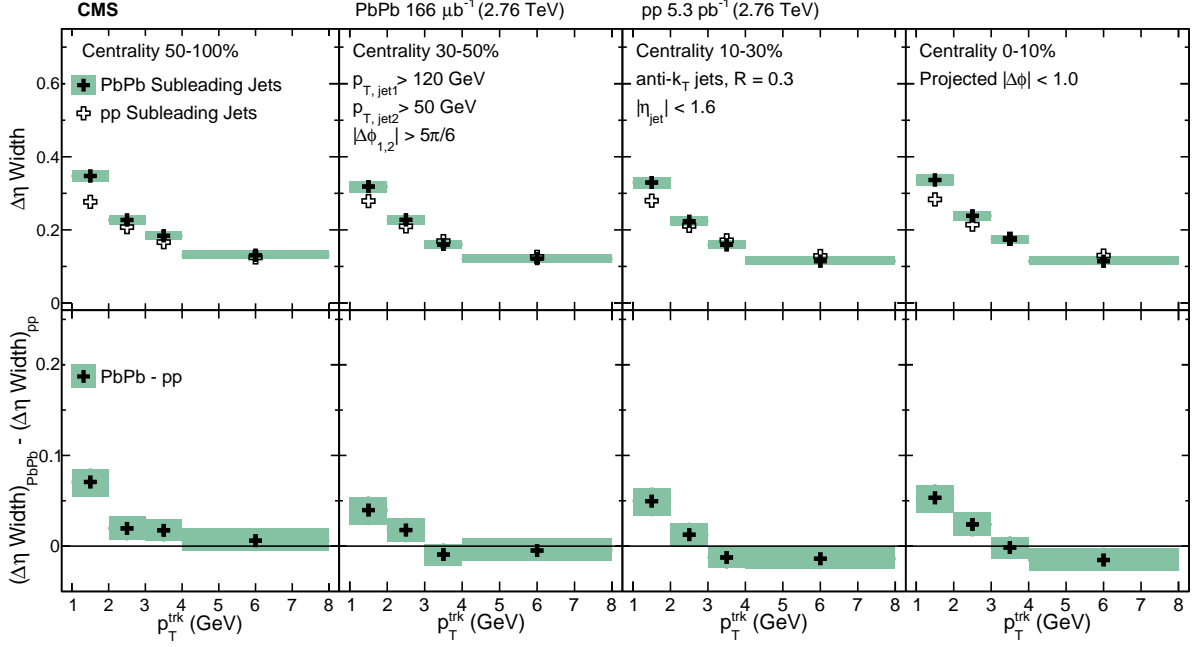


Figure 10: Comparison of the widths in PbPb and pp of the $\Delta\eta$ charged-particle distributions correlated to leading jets with $p_{T,\text{jet}2} > 50 \text{ GeV}$, as a function of p_T^{trk} . The bottom row shows the difference of the widths in PbPb and pp data. The shaded band corresponds to systematic uncertainty, and statistical uncertainties are smaller than symbol size.

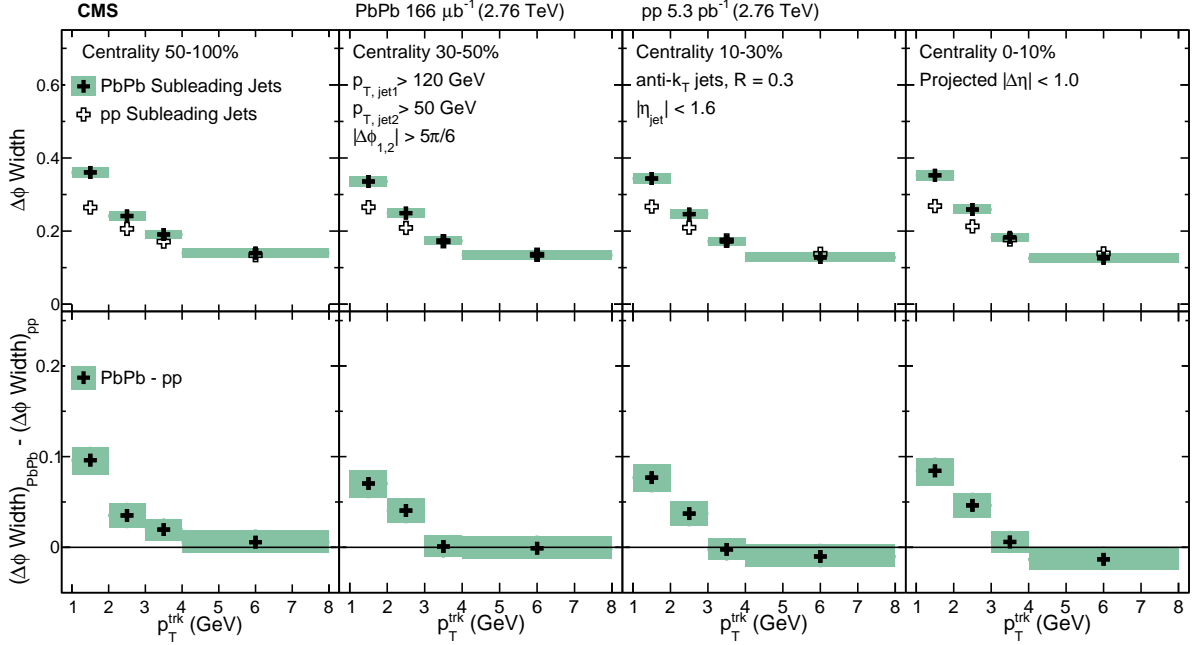


Figure 11: Comparison of the widths in PbPb and pp of the $\Delta\phi$ charged-particle distributions correlated to leading jets with $p_{T,\text{jet}2} > 50 \text{ GeV}$, as a function of p_T^{trk} . The bottom row shows the difference of the widths in PbPb and pp data. The shaded band corresponds to systematic uncertainty, and statistical uncertainties are smaller than symbol size.

large angles away from the jet axis.

Acknowledgments

We congratulate our colleagues in the CERN accelerator departments for the excellent performance of the LHC and thank the technical and administrative staffs at CERN and at other CMS institutes for their contributions to the success of the CMS effort. In addition, we gratefully acknowledge the computing centers and personnel of the Worldwide LHC Computing Grid for delivering so effectively the computing infrastructure essential to our analyses. Finally, we acknowledge the enduring support for the construction and operation of the LHC and the CMS detector provided by the following funding agencies: BMWFW and FWF (Austria); FNRS and FWO (Belgium); CNPq, CAPES, FAPERJ, and FAPESP (Brazil); MES (Bulgaria); CERN; CAS, MoST, and NSFC (China); COLCIENCIAS (Colombia); MSES and CSF (Croatia); RPF (Cyprus); MoER, ERC IUT and ERDF (Estonia); Academy of Finland, MEC, and HIP (Finland); CEA and CNRS/IN2P3 (France); BMBF, DFG, and HGF (Germany); GSRT (Greece); OTKA and NIH (Hungary); DAE and DST (India); IPM (Iran); SFI (Ireland); INFN (Italy); MSIP and NRF (Republic of Korea); LAS (Lithuania); MOE and UM (Malaysia); CINVESTAV, CONACYT, SEP, and UASLP-FAI (Mexico); MBIE (New Zealand); PAEC (Pakistan); MSHE and NSC (Poland); FCT (Portugal); JINR (Dubna); MON, RosAtom, RAS and RFBR (Russia); MESTD (Serbia); SEIDI and CPAN (Spain); Swiss Funding Agencies (Switzerland); MST (Taipei); ThEPCenter, IPST, STAR and NSTDA (Thailand); TUBITAK and TAEK (Turkey); NASU and SFFR (Ukraine); STFC (United Kingdom); DOE and NSF (USA).

Individuals have received support from the Marie-Curie program and the European Research Council and EPLANET (European Union); the Leventis Foundation; the A. P. Sloan Foundation; the Alexander von Humboldt Foundation; the Belgian Federal Science Policy Office; the Fonds pour la Formation à la Recherche dans l’Industrie et dans l’Agriculture (FRIA-Belgium); the Agentschap voor Innovatie door Wetenschap en Technologie (IWT-Belgium); the Ministry of Education, Youth and Sports (MEYS) of the Czech Republic; the Council of Science and Industrial Research, India; the HOMING PLUS program of the Foundation for Polish Science, cofinanced from European Union, Regional Development Fund; the OPUS program of the National Science Center (Poland); the Compagnia di San Paolo (Torino); MIUR project 20108T4XTM (Italy); the Thalis and Aristeia programs cofinanced by EU-ESF and the Greek NSRF; the National Priorities Research Program by Qatar National Research Fund; the Rachadapisek Sompot Fund for Postdoctoral Fellowship, Chulalongkorn University (Thailand); the Chulalongkorn Academic into Its 2nd Century Project Advancement Project (Thailand); and the Welch Foundation, contract C-1845.

References

- [1] J. D. Bjorken, “Energy loss of energetic partons in QGP: possible extinction of high p_T jets in hadron-hadron collisions”, (1982). FERMILAB-PUB-82-059-THY.
- [2] PHENIX Collaboration, “Suppression of hadrons with large transverse momentum in central Au+Au collisions at $\sqrt{s_{NN}} = 130 \text{ GeV}$ ”, *Phys. Rev. Lett.* **88** (2002) 022301, doi:10.1103/PhysRevLett.88.022301, arXiv:nucl-ex/0109003.
- [3] STAR Collaboration, “Centrality dependence of high p_T hadron suppression in Au+Au collisions at $\sqrt{s_{NN}} = 130 \text{ GeV}$ ”, *Phys. Rev. Lett.* **89** (2002) 202301, doi:10.1103/PhysRevLett.89.202301, arXiv:nucl-ex/0206011.

- [4] ALICE Collaboration, "Suppression of Charged Particle Production at Large Transverse Momentum in Central PbPb Collisions at $\sqrt{s_{NN}} = 2.76$ TeV", *Phys. Lett. B* **696** (2011) 30, doi:10.1016/j.physletb.2010.12.020, arXiv:1012.1004.
- [5] CMS Collaboration, "Study of high- p_T charged particle suppression in PbPb compared to pp collisions at $\sqrt{s_{NN}} = 2.76$ TeV", *Eur. Phys. J. C* **72** (2012) 1945, doi:10.1140/epjc/s10052-012-1945-x, arXiv:1202.2554.
- [6] ATLAS Collaboration, "Measurement of charged-particle spectra in Pb+Pb collisions at $\sqrt{s_{NN}} = 2.76$ TeV with the ATLAS detector at the LHC", *JHEP* **09** (2015) 050, doi:10.1007/JHEP09(2015)050, arXiv:1504.04337.
- [7] ATLAS Collaboration, "Observation of a Centrality-Dependent Dijet Asymmetry in Lead-Lead Collisions at $\sqrt{s_{NN}} = 2.76$ TeV with the ATLAS Detector at the LHC", *Phys. Rev. Lett.* **105** (2010) 252303, doi:10.1103/PhysRevLett.105.252303, arXiv:1011.6182.
- [8] CMS Collaboration, "Jet momentum dependence of jet quenching in PbPb collisions at $\sqrt{s_{NN}} = 2.76$ TeV", *Phys. Lett. B* **712** (2012) 176, doi:10.1016/j.physletb.2012.04.058, arXiv:1202.5022.
- [9] CMS Collaboration, "Studies of dijet transverse momentum balance and pseudorapidity distributions in pPb collisions at $\sqrt{s_{NN}} = 5.02$ TeV", *Eur. Phys. J. C.* **74** (2014) 2951, doi:10.1140/epjc/s10052-014-2951-y, arXiv:1401.4433.
- [10] CMS Collaboration, "Observation and studies of jet quenching in PbPb collisions at $\sqrt{s_{NN}} = 2.76$ TeV", *Phys. Rev. C* **84** (2011) 024906, doi:10.1103/PhysRevC.84.024906, arXiv:1102.1957.
- [11] G.-Y. Qin and B. Muller, "Explanation of Di-jet asymmetry in Pb+Pb collisions at the Large Hadron Collider", *Phys. Rev. Lett.* **106** (2011) 162302, doi:10.1103/PhysRevLett.106.162302, arXiv:1012.5280.
- [12] Y. He, I. Vitev, and B.-W. Zhang, "Next-to-leading order analysis of inclusive jet and di-jet production in heavy ion reactions at the Large Hadron Collider", (2011). arXiv:1105.2566. Submitted to *Phys. Lett. B*.
- [13] C. Young, B. Schenke, S. Jeon, and C. Gale, "Dijet asymmetry at the energies available at the CERN Large Hadron Collider", *Phys. Rev. C* **84** (2011) 024907, doi:10.1103/PhysRevC.84.024907, arXiv:1103.5769.
- [14] G.-L. Ma, "Dijet asymmetry in Pb+Pb collisions at $\sqrt{s_{NN}}=2.76$ TeV within a multiphase transport model", *Phys. Rev. C* **87** (2013), no. 6, 064901, doi:10.1103/PhysRevC.87.064901, arXiv:1304.2841.
- [15] STAR Collaboration, "Evidence from $d + \text{Au}$ Measurements for Final-State Suppression of High- p_T Hadrons in Au + Au Collisions at RHIC", *Phys. Rev. Lett.* **91** (2003) 072304, doi:10.1103/PhysRevLett.91.072304, arXiv:nucl-ex/0306024.
- [16] STAR Collaboration, "Distributions of Charged Hadrons Associated with High Transverse Momentum Particles in pp and Au + Au Collisions at $\sqrt{s_{NN}} = 200$ GeV", *Phys. Rev. Lett.* **95** (2005) 152301, doi:10.1103/PhysRevLett.95.152301, arXiv:nucl-ex/0501016.

- [17] STAR Collaboration, “Direct Observation of Dijets in Central Au+Au Collisions at $\sqrt{s_{NN}} = 200$ GeV”, *Phys. Rev. Lett.* **97** (2006) 162301,
`doi:10.1103/PhysRevLett.97.162301`, arXiv:[nucl-ex/0604018](#).
- [18] STAR Collaboration, “Jet-Hadron Correlations in $\sqrt{s_{NN}} = 200$ GeV p+p and Central Au+Au Collisions”, *Phys. Rev. Lett.* **112** (2014) 122301,
`doi:10.1103/PhysRevLett.112.122301`, arXiv:[1302.6184](#).
- [19] PHENIX Collaboration, “Transverse momentum and centrality dependence of dihadron correlations in Au+Au collisions at $\sqrt{s_{NN}} = 200$ GeV: Jet-quenching and the response of partonic matter”, *Phys. Rev. C* **77** (2008) 011901,
`doi:10.1103/PhysRevC.77.011901`, arXiv:[0705.3238](#).
- [20] A. Majumder and M. Van Leeuwen, “The Theory and Phenomenology of Perturbative QCD Based Jet Quenching”, *Prog. Part. Nucl. Phys. A* **66** (2011) 41,
`doi:10.1016/j.ppnp.2010.09.001`, arXiv:[1002.2206](#).
- [21] CMS Collaboration, “Measurement of jet fragmentation into charged particles in pp and PbPb collisions at $\sqrt{s_{NN}} = 2.76$ TeV”, *JHEP* **10** (2012) 087,
`doi:10.1007/JHEP10(2012)087`, arXiv:[1205.5872](#).
- [22] CMS Collaboration, “Modification of jet shapes in PbPb collisions at $\sqrt{s_{NN}} = 2.76$ TeV”, *Phys. Lett. B* **730** (2014) 243, `doi:10.1016/j.physletb.2014.01.042`, arXiv:[1310.0878](#).
- [23] CMS Collaboration, “Measurement of jet fragmentation in PbPb and pp collisions at $\sqrt{s_{NN}} = 2.76$ TeV”, *Phys. Rev. C* **90** (2014) 024908,
`doi:10.1103/PhysRevC.90.024908`, arXiv:[1406.0932](#).
- [24] CMS Collaboration, “Measurement of transverse momentum relative to dijet systems in PbPb and pp collisions at $\sqrt{s_{NN}} = 2.76$ TeV”, (2015). arXiv:[1509.09029](#). Accepted by JHEP.
- [25] L. Apolinario, N. Armesto, and L. Cunqueiro, “An analysis of the influence of background subtraction and quenching on jet observables in heavy-ion collisions”, *JHEP* **02** (2013) 022, `doi:10.1007/JHEP02(2013)022`, arXiv:[1211.1161](#).
- [26] A. Ayala, I. Dominguez, J. Jalilian-Marian, and M. E. Tejeda-Yeomans, “Jet asymmetry and momentum imbalance from $2 \rightarrow 2$ and $2 \rightarrow 3$ partonic processes in relativistic heavy-ion collisions”, *Phys. Rev. C* **92** (2015), no. 4, 044902,
`doi:10.1103/PhysRevC.92.044902`, arXiv:[1503.06889](#).
- [27] J.-P. Blaizot, Y. Mehtar-Tani, and M. A. C. Torres, “Angular structure of the in-medium QCD cascade”, *Phys. Rev. Lett.* **114** (2015), no. 22, 222002,
`doi:10.1103/PhysRevLett.114.222002`, arXiv:[1407.0326](#).
- [28] CMS Collaboration, “Long-range and short-range dihadron angular correlations in central PbPb collisions at a nucleon-nucleon center of mass energy of 2.76 TeV”, *JHEP* **07** (2011) 076, `doi:10.1007/JHEP07(2011)076`, arXiv:[1105.2438](#).
- [29] B. Alver and G. Roland, “Collision geometry fluctuations and triangular flow in heavy-ion collisions”, *Phys. Rev. C* **81** (2010) 054905,
`doi:10.1103/PhysRevC.81.054905`, arXiv:[1003.0194](#). [Erratum: *Phys. Rev.C82,039903(2010)*].

- [30] CMS Collaboration, “Determination of Jet Energy Calibration and Transverse Momentum Resolution in CMS”, *JINST* **6** (2011) P11002, doi:10.1088/1748-0221/6/11/P11002, arXiv:1107.4277.
- [31] CMS Collaboration, “Performance of photon reconstruction and identification with the CMS detector in proton-proton collisions at $\sqrt{s} = 8 \text{ TeV}$ ”, *JINST* **10** (2015) P08010, doi:10.1088/1748-0221/10/08/P08010, arXiv:1502.02702.
- [32] CMS Collaboration, “Description and performance of track and primary-vertex reconstruction with the CMS tracker”, *JINST* **9** (2014) P10009, doi:10.1088/1748-0221/9/10/P10009, arXiv:1405.6569.
- [33] CMS Collaboration, “The CMS experiment at the CERN LHC”, *JINST* **3** (2008) S08004, doi:10.1088/1748-0221/3/08/S08004.
- [34] M. Cacciari, G. P. Salam, and G. Soyez, “The anti- k_t jet clustering algorithm”, *JHEP* **04** (2008) 063, doi:10.1088/1126-6708/2008/04/063, arXiv:0802.1189.
- [35] M. Cacciari, G. P. Salam, and G. Soyez, “FastJet user manual”, *Eur. Phys. J. C* **72** (2012) 1896, doi:10.1140/epjc/s10052-012-1896-2, arXiv:1111.6097.
- [36] CMS Collaboration, “Underlying-Event Subtraction for Particle Flow”, CMS Detector Performance Summary CMS-DP-2013-018, 2013.
- [37] T. Sjöstrand, S. Mrenna, and P. Skands, “PYTHIA 6.4 physics and manual”, *JHEP* **05** (2006) 026, doi:10.1088/1126-6708/2006/05/026, arXiv:hep-ph/0603175.
- [38] R. Field, “Early LHC Underlying Event Data - Findings and Surprises”, in *Hadron collider physics. Proceedings, 22nd Conference, HCP 2010, Toronto, Canada*. 2010. arXiv:1010.3558.
- [39] GEANT4 Collaboration, “GEANT4—a simulation toolkit”, *Nucl. Instrum. Meth. A* **506** (2003) 250, doi:10.1016/S0168-9002(03)01368-8.
- [40] I. P. Lokhtin and A. M. Snigirev, “A model of jet quenching in ultrarelativistic heavy ion collisions and high- p_T hadron spectra at RHIC”, *Eur. Phys. J. C* **45** (2006) 211, doi:10.1140/epjc/s2005-02426-3, arXiv:hep-ph/0506189.
- [41] CMS Collaboration, “Studies of jet quenching using isolated-photon+jet correlations in PbPb and pp collisions at $\sqrt{s_{NN}} = 2.76 \text{ TeV}$ ”, *Phys. Lett. B* **718** (2013) 773, doi:10.1016/j.physletb.2012.11.003, arXiv:1205.0206.
- [42] CMS Collaboration, “Multiplicity and transverse momentum dependence of long-range correlations in pPb collisions”, *Phys. Lett. B* **724** (2013) 213, doi:10.1016/j.physletb.2013.06.028, arXiv:1305.0609.
- [43] CMS Collaboration, “Observation of long-range, near-side angular correlations in proton-proton collisions at the LHC”, *J. High Energy Phys.* **09** (2010) 091, doi:10.1007/JHEP09(2010)091.
- [44] CMS Collaboration, “Observation of long-range, near-side angular correlations in pPb collisions at the LHC.”, *Phys. Lett. B* **718** (2013) 795, doi:10.1016/j.physletb.2012.11.025, arXiv:1210.5482.

- [45] CMS Collaboration, “Azimuthal Anisotropy of Charge Particles at High Transvere
Momenta in Pb-Pb Collisions at $\sqrt{s_{NN}} = 2.76$ TeV”, *Phys. Rev. Lett.* **109** (2012) 022301,
[doi:10.1103/PhysRevLett.109.022301](https://doi.org/10.1103/PhysRevLett.109.022301), arXiv:1204.1850.

A The CMS Collaboration

Yerevan Physics Institute, Yerevan, Armenia
V. Khachatryan, A.M. Sirunyan, A. Tumasyan

Institut für Hochenergiephysik der OeAW, Wien, Austria

W. Adam, E. Asilar, T. Bergauer, J. Brandstetter, E. Brondolin, M. Dragicevic, J. Erö, M. Flechl, M. Friedl, R. Frühwirth¹, V.M. Ghete, C. Hartl, N. Hörmann, J. Hrubec, M. Jeitler¹, V. Knünz, A. König, M. Krammer¹, I. Krätschmer, D. Liko, T. Matsushita, I. Mikulec, D. Rabady², N. Rad, B. Rahbaran, H. Rohringer, J. Schieck¹, R. Schöfbeck, J. Strauss, W. Treberer-Treberspurg, W. Waltenberger, C.-E. Wulz¹

National Centre for Particle and High Energy Physics, Minsk, Belarus

V. Mossolov, N. Shumeiko, J. Suarez Gonzalez

Universiteit Antwerpen, Antwerpen, Belgium

S. Alderweireldt, T. Cornelis, E.A. De Wolf, X. Janssen, A. Knutsson, J. Lauwers, S. Luyckx, M. Van De Klundert, H. Van Haevermaet, P. Van Mechelen, N. Van Remortel, A. Van Spilbeeck

Vrije Universiteit Brussel, Brussel, Belgium

S. Abu Zeid, F. Blekman, J. D'Hondt, N. Daci, I. De Bruyn, K. Deroover, N. Heracleous, J. Keaveney, S. Lowette, L. Moreels, A. Olbrechts, Q. Python, D. Strom, S. Tavernier, W. Van Doninck, P. Van Mulders, G.P. Van Onsem, I. Van Parijs

Université Libre de Bruxelles, Bruxelles, Belgium

P. Barria, H. Brun, C. Caillol, B. Clerbaux, G. De Lentdecker, G. Fasanella, L. Favart, R. Goldouzian, A. Grebenyuk, G. Karapostoli, T. Lenzi, A. Léonard, T. Maerschalk, A. Marinov, L. Perniè, A. Randle-conde, T. Seva, C. Vander Velde, P. Vanlaer, R. Yonamine, F. Zenoni, F. Zhang³

Ghent University, Ghent, Belgium

K. Beernaert, L. Benucci, A. Cimmino, S. Crucy, D. Dobur, A. Fagot, G. Garcia, M. Gul, J. Mccartin, A.A. Ocampo Rios, D. Poyraz, D. Ryckbosch, S. Salva, M. Sigamani, M. Tytgat, W. Van Driessche, E. Yazgan, N. Zaganidis

Université Catholique de Louvain, Louvain-la-Neuve, Belgium

S. Basegmez, C. Beluffi⁴, O. Bondu, S. Brochet, G. Bruno, A. Caudron, L. Ceard, C. Delaere, D. Favart, L. Forthomme, A. Giannanco⁵, A. Jafari, P. Jez, M. Komm, V. Lemaitre, A. Mertens, M. Musich, C. Nuttens, L. Perrini, K. Piotrzkowski, A. Popov⁶, L. Quertenmont, M. Selvaggi, M. Vidal Marono

Université de Mons, Mons, Belgium

N. Belyi, G.H. Hammad

Centro Brasileiro de Pesquisas Fisicas, Rio de Janeiro, Brazil

W.L. Aldá Júnior, F.L. Alves, G.A. Alves, L. Brito, M. Correa Martins Junior, M. Hamer, C. Hensel, A. Moraes, M.E. Pol, P. Rebello Teles

Universidade do Estado do Rio de Janeiro, Rio de Janeiro, Brazil

E. Belchior Batista Das Chagas, W. Carvalho, J. Chinellato⁷, A. Custódio, E.M. Da Costa, D. De Jesus Damiao, C. De Oliveira Martins, S. Fonseca De Souza, L.M. Huertas Guativa, H. Malbouisson, D. Matos Figueiredo, C. Mora Herrera, L. Mundim, H. Nogima, W.L. Prado Da Silva, A. Santoro, A. Sznajder, E.J. Tonelli Manganote⁷, A. Vilela Pereira

Universidade Estadual Paulista ^a, Universidade Federal do ABC ^b, São Paulo, Brazil
 S. Ahuja^a, C.A. Bernardes^b, A. De Souza Santos^b, S. Dogra^a, T.R. Fernandez Perez Tomei^a,
 E.M. Gregores^b, P.G. Mercadante^b, C.S. Moon^{a,8}, S.F. Novaes^a, Sandra S. Padula^a, D. Romero
 Abad, J.C. Ruiz Vargas

Institute for Nuclear Research and Nuclear Energy, Sofia, Bulgaria

A. Aleksandrov, R. Hadjiiska, P. Iaydjiev, M. Rodozov, S. Stoykova, G. Sultanov, M. Vutova

University of Sofia, Sofia, Bulgaria

A. Dimitrov, I. Glushkov, L. Litov, B. Pavlov, P. Petkov

Institute of High Energy Physics, Beijing, China

M. Ahmad, J.G. Bian, G.M. Chen, H.S. Chen, M. Chen, T. Cheng, R. Du, C.H. Jiang, D. Leggat,
 R. Plestina⁹, F. Romeo, S.M. Shaheen, A. Spiezia, J. Tao, C. Wang, Z. Wang, H. Zhang

State Key Laboratory of Nuclear Physics and Technology, Peking University, Beijing, China

C. Asawatangtrakuldee, Y. Ban, Q. Li, S. Liu, Y. Mao, S.J. Qian, D. Wang, Z. Xu

Universidad de Los Andes, Bogota, Colombia

C. Avila, A. Cabrera, L.F. Chaparro Sierra, C. Florez, J.P. Gomez, B. Gomez Moreno,
 J.C. Sanabria

**University of Split, Faculty of Electrical Engineering, Mechanical Engineering and Naval
 Architecture, Split, Croatia**

N. Godinovic, D. Lelas, I. Puljak, P.M. Ribeiro Cipriano

University of Split, Faculty of Science, Split, Croatia

Z. Antunovic, M. Kovac

Institute Rudjer Boskovic, Zagreb, Croatia

V. Brigljevic, K. Kadija, J. Luetic, S. Micanovic, L. Sudic

University of Cyprus, Nicosia, Cyprus

A. Attikis, G. Mavromanolakis, J. Mousa, C. Nicolaou, F. Ptochos, P.A. Razis, H. Rykaczewski

Charles University, Prague, Czech Republic

M. Bodlak, M. Finger¹⁰, M. Finger Jr.¹⁰

**Academy of Scientific Research and Technology of the Arab Republic of Egypt, Egyptian
 Network of High Energy Physics, Cairo, Egypt**

A.A. Abdelalim^{11,12}, A. Awad, A. Mahrous¹¹, A. Radi^{13,14}

National Institute of Chemical Physics and Biophysics, Tallinn, Estonia

B. Calpas, M. Kadastik, M. Murumaa, M. Raidal, A. Tiko, C. Veelken

Department of Physics, University of Helsinki, Helsinki, Finland

P. Eerola, J. Pekkanen, M. Voutilainen

Helsinki Institute of Physics, Helsinki, Finland

J. Hätkönen, V. Karimäki, R. Kinnunen, T. Lampén, K. Lassila-Perini, S. Lehti, T. Lindén,
 P. Luukka, T. Peltola, E. Tuominen, J. Tuominiemi, E. Tuovinen, L. Wendland

Lappeenranta University of Technology, Lappeenranta, Finland

J. Talvitie, T. Tuuva

DSM/IRFU, CEA/Saclay, Gif-sur-Yvette, France

M. Besancon, F. Couderc, M. Dejardin, D. Denegri, B. Fabbro, J.L. Faure, C. Favaro, F. Ferri,

S. Ganjour, A. Givernaud, P. Gras, G. Hamel de Monchenault, P. Jarry, E. Locci, M. Machet, J. Malcles, J. Rander, A. Rosowsky, M. Titov, A. Zghiche

Laboratoire Leprince-Ringuet, Ecole Polytechnique, IN2P3-CNRS, Palaiseau, France

I. Antropov, S. Baffioni, F. Beaudette, P. Busson, L. Cadamuro, E. Chapon, C. Charlot, O. Davignon, N. Filipovic, R. Granier de Cassagnac, M. Jo, S. Lisniak, L. Mastrolorenzo, P. Miné, I.N. Naranjo, M. Nguyen, C. Ochando, G. Ortona, P. Paganini, P. Pigard, S. Regnard, R. Salerno, J.B. Sauvan, Y. Sirois, T. Strebler, Y. Yilmaz, A. Zabi

Institut Pluridisciplinaire Hubert Curien, Université de Strasbourg, Université de Haute Alsace Mulhouse, CNRS/IN2P3, Strasbourg, France

J.-L. Agram¹⁵, J. Andrea, A. Aubin, D. Bloch, J.-M. Brom, M. Buttignol, E.C. Chabert, N. Chanon, C. Collard, E. Conte¹⁵, X. Coubez, J.-C. Fontaine¹⁵, D. Gelé, U. Goerlach, C. Goetzmann, A.-C. Le Bihan, J.A. Merlin², K. Skovpen, P. Van Hove

Centre de Calcul de l’Institut National de Physique Nucléaire et de Physique des Particules, CNRS/IN2P3, Villeurbanne, France

S. Gadrat

Université de Lyon, Université Claude Bernard Lyon 1, CNRS-IN2P3, Institut de Physique Nucléaire de Lyon, Villeurbanne, France

S. Beauceron, C. Bernet, G. Boudoul, E. Bouvier, C.A. Carrillo Montoya, R. Chierici, D. Contardo, B. Courbon, P. Depasse, H. El Mamouni, J. Fan, J. Fay, S. Gascon, M. Gouzevitch, B. Ille, F. Lagarde, I.B. Laktineh, M. Lethuillier, L. Mirabito, A.L. Pequegnot, S. Perries, J.D. Ruiz Alvarez, D. Sabes, L. Sgandurra, V. Sordini, M. Vander Donckt, P. Verdier, S. Viret

Georgian Technical University, Tbilisi, Georgia

T. Toriashvili¹⁶

Tbilisi State University, Tbilisi, Georgia

Z. Tsamalaidze¹⁰

RWTH Aachen University, I. Physikalisches Institut, Aachen, Germany

C. Autermann, S. Beranek, L. Feld, A. Heister, M.K. Kiesel, K. Klein, M. Lipinski, A. Ostapchuk, M. Preuten, F. Raupach, S. Schael, J.F. Schulte, T. Verlage, H. Weber, V. Zhukov⁶

RWTH Aachen University, III. Physikalisches Institut A, Aachen, Germany

M. Ata, M. Brodski, E. Dietz-Laursonn, D. Duchardt, M. Endres, M. Erdmann, S. Erdweg, T. Esch, R. Fischer, A. Güth, T. Hebbeker, C. Heidemann, K. Hoepfner, S. Knutzen, P. Kreuzer, M. Merschmeyer, A. Meyer, P. Millet, S. Mukherjee, M. Olszewski, K. Padeken, P. Papacz, T. Pook, M. Radziej, H. Reithler, M. Rieger, F. Scheuch, L. Sonnenschein, D. Teyssier, S. Thüer

RWTH Aachen University, III. Physikalisches Institut B, Aachen, Germany

V. Cherepanov, Y. Erdogan, G. Flügge, H. Geenen, M. Geisler, F. Hoehle, B. Kargoll, T. Kress, A. Künsken, J. Lingemann, A. Nehrkorn, A. Nowack, I.M. Nugent, C. Pistone, O. Pooth, A. Stahl

Deutsches Elektronen-Synchrotron, Hamburg, Germany

M. Aldaya Martin, I. Asin, N. Bartosik, O. Behnke, U. Behrens, K. Borras¹⁷, A. Burgmeier, A. Campbell, C. Contreras-Campana, F. Costanza, C. Diez Pardos, G. Dolinska, S. Dooling, T. Dorland, G. Eckerlin, D. Eckstein, T. Eichhorn, G. Flucke, E. Gallo¹⁸, J. Garay Garcia, A. Geiser, A. Gzhko, P. Gunnellini, J. Hauk, M. Hempel¹⁹, H. Jung, A. Kalogeropoulos, O. Karacheban¹⁹, M. Kasemann, P. Katsas, J. Kieseler, C. Kleinwort, I. Korol, W. Lange, J. Leonard, K. Lipka, A. Lobanov, W. Lohmann¹⁹, R. Mankel, I.-A. Melzer-Pellmann,

A.B. Meyer, G. Mittag, J. Mnich, A. Mussgiller, S. Naumann-Emme, A. Nayak, E. Ntomari, H. Perrey, D. Pitzl, R. Placakyte, A. Raspereza, B. Roland, M.Ö. Sahin, P. Saxena, T. Schoerner-Sadenius, C. Seitz, S. Spannagel, K.D. Trippkewitz, R. Walsh, C. Wissing

University of Hamburg, Hamburg, Germany

V. Blobel, M. Centis Vignali, A.R. Draeger, J. Erfle, E. Garutti, K. Goebel, D. Gonzalez, M. Görner, J. Haller, M. Hoffmann, R.S. Höing, A. Junkes, R. Klanner, R. Kogler, N. Kovalchuk, T. Lapsien, T. Lenz, I. Marchesini, D. Marconi, M. Meyer, D. Nowatschin, J. Ott, F. Pantaleo², T. Peiffer, A. Perieanu, N. Pietsch, J. Poehlsen, D. Rathjens, C. Sander, C. Scharf, P. Schleper, E. Schlieckau, A. Schmidt, S. Schumann, J. Schwandt, V. Sola, H. Stadie, G. Steinbrück, F.M. Stober, H. Tholen, D. Troendle, E. Usai, L. Vanelderden, A. Vanhoefer, B. Vormwald

Institut für Experimentelle Kernphysik, Karlsruhe, Germany

C. Barth, C. Baus, J. Berger, C. Böser, E. Butz, T. Chwalek, F. Colombo, W. De Boer, A. Descroix, A. Dierlamm, S. Fink, F. Frensch, R. Friese, M. Giffels, A. Gilbert, D. Haitz, F. Hartmann², S.M. Heindl, U. Husemann, I. Katkov⁶, A. Kornmayer², P. Lobelle Pardo, B. Maier, H. Mildner, M.U. Mozer, T. Müller, Th. Müller, M. Plagge, G. Quast, K. Rabbertz, S. Röcker, F. Roscher, M. Schröder, G. Sieber, H.J. Simonis, R. Ulrich, J. Wagner-Kuhr, S. Wayand, M. Weber, T. Weiler, S. Williamson, C. Wöhrmann, R. Wolf

Institute of Nuclear and Particle Physics (INPP), NCSR Demokritos, Aghia Paraskevi, Greece

G. Anagnostou, G. Daskalakis, T. Geralis, V.A. Giakoumopoulou, A. Kyriakis, D. Loukas, A. Psallidas, I. Topsis-Giotis

National and Kapodistrian University of Athens, Athens, Greece

A. Agapitos, S. Kesisoglou, A. Panagiotou, N. Saoulidou, E. Tziaferi

University of Ioánnina, Ioánnina, Greece

I. Evangelou, G. Flouris, C. Foudas, P. Kokkas, N. Loukas, N. Manthos, I. Papadopoulos, E. Paradas, J. Strologas

Wigner Research Centre for Physics, Budapest, Hungary

G. Bencze, C. Hajdu, A. Hazi, P. Hidas, D. Horvath²⁰, F. Sikler, V. Veszpremi, G. Vesztergombi²¹, A.J. Zsigmond

Institute of Nuclear Research ATOMKI, Debrecen, Hungary

N. Beni, S. Czellar, J. Karancsi²², J. Molnar, Z. Szillasi²

University of Debrecen, Debrecen, Hungary

M. Bartók²³, A. Makovec, P. Raics, Z.L. Trocsanyi, B. Ujvari

National Institute of Science Education and Research, Bhubaneswar, India

S. Choudhury²⁴, P. Mal, K. Mandal, D.K. Sahoo, N. Sahoo, S.K. Swain

Panjab University, Chandigarh, India

S. Bansal, S.B. Beri, V. Bhatnagar, R. Chawla, R. Gupta, U.Bhawandeep, A.K. Kalsi, A. Kaur, M. Kaur, R. Kumar, A. Mehta, M. Mittal, J.B. Singh, G. Walia

University of Delhi, Delhi, India

Ashok Kumar, A. Bhardwaj, B.C. Choudhary, R.B. Garg, S. Malhotra, M. Naimuddin, N. Nishu, K. Ranjan, R. Sharma, V. Sharma

Saha Institute of Nuclear Physics, Kolkata, India

S. Bhattacharya, K. Chatterjee, S. Dey, S. Dutta, N. Majumdar, A. Modak, K. Mondal, S. Mukhopadhyay, A. Roy, D. Roy, S. Roy Chowdhury, S. Sarkar, M. Sharan

Bhabha Atomic Research Centre, Mumbai, India

A. Abdulsalam, R. Chudasama, D. Dutta, V. Jha, V. Kumar, A.K. Mohanty², L.M. Pant, P. Shukla, A. Topkar

Tata Institute of Fundamental Research, Mumbai, India

T. Aziz, S. Banerjee, S. Bhowmik²⁵, R.M. Chatterjee, R.K. Dewanjee, S. Dugad, S. Ganguly, S. Ghosh, M. Guchait, A. Gurtu²⁶, Sa. Jain, G. Kole, S. Kumar, B. Mahakud, M. Maity²⁵, G. Majumder, K. Mazumdar, S. Mitra, G.B. Mohanty, B. Parida, T. Sarkar²⁵, N. Sur, B. Sutar, N. Wickramage²⁷

Indian Institute of Science Education and Research (IISER), Pune, India

S. Chauhan, S. Dube, A. Kapoor, K. Kothekar, S. Sharma

Institute for Research in Fundamental Sciences (IPM), Tehran, Iran

H. Bakhshiansohi, H. Behnamian, S.M. Etesami²⁸, A. Fahim²⁹, M. Khakzad, M. Mohammadi Najafabadi, M. Naseri, S. Paktnat Mehdiabadi, F. Rezaei Hosseinabadi, B. Safarzadeh³⁰, M. Zeinali

University College Dublin, Dublin, Ireland

M. Felcini, M. Grunewald

INFN Sezione di Bari ^a, Università di Bari ^b, Politecnico di Bari ^c, Bari, Italy

M. Abbrescia^{a,b}, C. Calabria^{a,b}, C. Caputo^{a,b}, A. Colaleo^a, D. Creanza^{a,c}, L. Cristella^{a,b}, N. De Filippis^{a,c}, M. De Palma^{a,b}, L. Fiore^a, G. Iaselli^{a,c}, G. Maggi^{a,c}, M. Maggi^a, G. Miniello^{a,b}, S. My^{a,c}, S. Nuzzo^{a,b}, A. Pompili^{a,b}, G. Pugliese^{a,c}, R. Radogna^{a,b}, A. Ranieri^a, G. Selvaggi^{a,b}, L. Silvestris^{a,2}, R. Venditti^{a,b}

INFN Sezione di Bologna ^a, Università di Bologna ^b, Bologna, Italy

G. Abbiendi^a, C. Battilana², A.C. Benvenuti^a, D. Bonacorsi^{a,b}, S. Braibant-Giacomelli^{a,b}, L. Brigliadori^{a,b}, R. Campanini^{a,b}, P. Capiluppi^{a,b}, A. Castro^{a,b}, F.R. Cavallo^a, S.S. Chhibra^{a,b}, G. Codispoti^{a,b}, M. Cuffiani^{a,b}, G.M. Dallavalle^a, F. Fabbri^a, A. Fanfani^{a,b}, D. Fasanella^{a,b}, P. Giacomelli^a, C. Grandi^a, L. Guiducci^{a,b}, S. Marcellini^a, G. Masetti^a, A. Montanari^a, F.L. Navarria^{a,b}, A. Perrotta^a, A.M. Rossi^{a,b}, T. Rovelli^{a,b}, G.P. Siroli^{a,b}, N. Tosi^{a,b,2}, R. Travaglini^{a,b}

INFN Sezione di Catania ^a, Università di Catania ^b, Catania, Italy

G. Cappello^a, M. Chiorboli^{a,b}, S. Costa^{a,b}, A. Di Mattia^a, F. Giordano^{a,b}, R. Potenza^{a,b}, A. Tricomi^{a,b}, C. Tuve^{a,b}

INFN Sezione di Firenze ^a, Università di Firenze ^b, Firenze, Italy

G. Barbagli^a, V. Ciulli^{a,b}, C. Civinini^a, R. D'Alessandro^{a,b}, E. Focardi^{a,b}, V. Gori^{a,b}, P. Lenzi^{a,b}, M. Meschini^a, S. Paoletti^a, G. Sguazzoni^a, L. Viliani^{a,b,2}

INFN Laboratori Nazionali di Frascati, Frascati, Italy

L. Benussi, S. Bianco, F. Fabbri, D. Piccolo, F. Primavera²

INFN Sezione di Genova ^a, Università di Genova ^b, Genova, Italy

V. Calvelli^{a,b}, F. Ferro^a, M. Lo Vetere^{a,b}, M.R. Monge^{a,b}, E. Robutti^a, S. Tosi^{a,b}

INFN Sezione di Milano-Bicocca ^a, Università di Milano-Bicocca ^b, Milano, Italy

L. Brianza, M.E. Dinardo^{a,b}, S. Fiorendi^{a,b}, S. Gennai^a, R. Gerosa^{a,b}, A. Ghezzi^{a,b}, P. Govoni^{a,b},

S. Malvezzi^a, R.A. Manzoni^{a,b,2}, B. Marzocchi^{a,b}, D. Menasce^a, L. Moroni^a, M. Paganoni^{a,b}, D. Pedrini^a, S. Ragazzi^{a,b}, N. Redaelli^a, T. Tabarelli de Fatis^{a,b}

INFN Sezione di Napoli ^a, **Università di Napoli 'Federico II'** ^b, **Napoli, Italy**, **Università della Basilicata** ^c, **Potenza, Italy**, **Università G. Marconi** ^d, **Roma, Italy**

S. Buontempo^a, N. Cavallo^{a,c}, S. Di Guida^{a,d,2}, M. Esposito^{a,b}, F. Fabozzi^{a,c}, A.O.M. Iorio^{a,b}, G. Lanza^a, L. Lista^a, S. Meola^{a,d,2}, M. Merola^a, P. Paolucci^{a,2}, C. Sciacca^{a,b}, F. Thyssen

INFN Sezione di Padova ^a, **Università di Padova** ^b, **Padova, Italy**, **Università di Trento** ^c, **Trento, Italy**

P. Azzi^{a,2}, N. Bacchetta^a, L. Benato^{a,b}, D. Bisello^{a,b}, A. Boletti^{a,b}, R. Carlin^{a,b}, P. Checchia^a, M. Dall'Osso^{a,b,2}, T. Dorigo^a, U. Dosselli^a, F. Gasparini^{a,b}, U. Gasparini^{a,b}, A. Gozzelino^a, S. Lacaprara^a, M. Margoni^{a,b}, A.T. Meneguzzo^{a,b}, J. Pazzini^{a,b,2}, M. Pegoraro^a, N. Pozzobon^{a,b}, P. Ronchese^{a,b}, F. Simonetto^{a,b}, E. Torassa^a, M. Tosi^{a,b}, S. Vanini^{a,b}, S. Ventura^a, M. Zanetti, P. Zotto^{a,b}, A. Zucchetta^{a,b,2}, G. Zumerle^{a,b}

INFN Sezione di Pavia ^a, **Università di Pavia** ^b, **Pavia, Italy**

A. Braghieri^a, A. Magnani^{a,b}, P. Montagna^{a,b}, S.P. Ratti^{a,b}, V. Re^a, C. Riccardi^{a,b}, P. Salvini^a, I. Vai^{a,b}, P. Vitulo^{a,b}

INFN Sezione di Perugia ^a, **Università di Perugia** ^b, **Perugia, Italy**

L. Alunni Solestizi^{a,b}, G.M. Bilei^a, D. Ciangottini^{a,b,2}, L. Fanò^{a,b}, P. Lariccia^{a,b}, G. Mantovani^{a,b}, M. Menichelli^a, A. Saha^a, A. Santocchia^{a,b}

INFN Sezione di Pisa ^a, **Università di Pisa** ^b, **Scuola Normale Superiore di Pisa** ^c, **Pisa, Italy**

K. Androsov^{a,31}, P. Azzurri^{a,2}, G. Bagliesi^a, J. Bernardini^a, T. Boccali^a, R. Castaldi^a, M.A. Ciocci^{a,31}, R. Dell'Orso^a, S. Donato^{a,c,2}, G. Fedi, L. Foà^{a,c†}, A. Giassi^a, M.T. Grippo^{a,31}, F. Ligabue^{a,c}, T. Lomtadze^a, L. Martini^{a,b}, A. Messineo^{a,b}, F. Palla^a, A. Rizzi^{a,b}, A. Savoy-Navarro^{a,32}, A.T. Serban^a, P. Spagnolo^a, R. Tenchini^a, G. Tonelli^{a,b}, A. Venturi^a, P.G. Verdini^a

INFN Sezione di Roma ^a, **Università di Roma** ^b, **Roma, Italy**

L. Barone^{a,b}, F. Cavallari^a, G. D'imperio^{a,b,2}, D. Del Re^{a,b,2}, M. Diemoz^a, S. Gelli^{a,b}, C. Jorda^a, E. Longo^{a,b}, F. Margaroli^{a,b}, P. Meridiani^a, G. Organtini^{a,b}, R. Paramatti^a, F. Preiato^{a,b}, S. Rahatlou^{a,b}, C. Rovelli^a, F. Santanastasio^{a,b}, P. Traczyk^{a,b,2}

INFN Sezione di Torino ^a, **Università di Torino** ^b, **Torino, Italy**, **Università del Piemonte Orientale** ^c, **Novara, Italy**

N. Amapane^{a,b}, R. Arcidiacono^{a,c,2}, S. Argiro^{a,b}, M. Arneodo^{a,c}, R. Bellan^{a,b}, C. Biino^a, N. Cartiglia^a, M. Costa^{a,b}, R. Covarelli^{a,b}, A. Degano^{a,b}, N. Demaria^a, L. Finco^{a,b,2}, B. Kiani^{a,b}, C. Mariotti^a, S. Maselli^a, E. Migliore^{a,b}, V. Monaco^{a,b}, E. Monteil^{a,b}, M.M. Obertino^{a,b}, L. Pacher^{a,b}, N. Pastrone^a, M. Pelliccioni^a, G.L. Pinna Angioni^{a,b}, F. Ravera^{a,b}, A. Romero^{a,b}, M. Ruspa^{a,c}, R. Sacchi^{a,b}, A. Solano^{a,b}, A. Staiano^a

INFN Sezione di Trieste ^a, **Università di Trieste** ^b, **Trieste, Italy**

S. Belforte^a, V. Candelise^{a,b}, M. Casarsa^a, F. Cossutti^a, G. Della Ricca^{a,b}, B. Gobbo^a, C. La Licata^{a,b}, M. Marone^{a,b}, A. Schizzi^{a,b}, A. Zanetti^a

Kangwon National University, Chunchon, Korea

A. Kropivnitskaya, S.K. Nam

Kyungpook National University, Daegu, Korea

D.H. Kim, G.N. Kim, M.S. Kim, D.J. Kong, S. Lee, Y.D. Oh, A. Sakharov, D.C. Son

Chonbuk National University, Jeonju, Korea

J.A. Brochero Cifuentes, H. Kim, T.J. Kim

Chonnam National University, Institute for Universe and Elementary Particles, Kwangju, Korea

S. Song

Korea University, Seoul, Korea

S. Choi, Y. Go, D. Gyung, B. Hong, H. Kim, Y. Kim, B. Lee, K. Lee, K.S. Lee, S. Lee, S.K. Park, Y. Roh

Seoul National University, Seoul, Korea

H.D. Yoo

University of Seoul, Seoul, Korea

M. Choi, H. Kim, J.H. Kim, J.S.H. Lee, I.C. Park, G. Ryu, M.S. Ryu

Sungkyunkwan University, Suwon, Korea

Y. Choi, J. Goh, D. Kim, E. Kwon, J. Lee, I. Yu

Vilnius University, Vilnius, Lithuania

V. Dudenas, A. Juodagalvis, J. Vaitkus

National Centre for Particle Physics, Universiti Malaya, Kuala Lumpur, Malaysia

I. Ahmed, Z.A. Ibrahim, J.R. Komaragiri, M.A.B. Md Ali³³, F. Mohamad Idris³⁴, W.A.T. Wan Abdullah, M.N. Yusli

Centro de Investigacion y de Estudios Avanzados del IPN, Mexico City, Mexico

E. Casimiro Linares, H. Castilla-Valdez, E. De La Cruz-Burelo, I. Heredia-De La Cruz³⁵, A. Hernandez-Almada, R. Lopez-Fernandez, A. Sanchez-Hernandez

Universidad Iberoamericana, Mexico City, Mexico

S. Carrillo Moreno, F. Vazquez Valencia

Benemerita Universidad Autonoma de Puebla, Puebla, Mexico

I. Pedraza, H.A. Salazar Ibarguen

Universidad Autónoma de San Luis Potosí, San Luis Potosí, Mexico

A. Morelos Pineda

University of Auckland, Auckland, New Zealand

D. Kofcheck

University of Canterbury, Christchurch, New Zealand

P.H. Butler

National Centre for Physics, Quaid-I-Azam University, Islamabad, Pakistan

A. Ahmad, M. Ahmad, Q. Hassan, H.R. Hoorani, W.A. Khan, T. Khurshid, M. Shoaib

National Centre for Nuclear Research, Swierk, Poland

H. Bialkowska, M. Bluj, B. Boimska, T. Frueboes, M. Górska, M. Kazana, K. Nawrocki, K. Romanowska-Rybinska, M. Szleper, P. Zalewski

Institute of Experimental Physics, Faculty of Physics, University of Warsaw, Warsaw, Poland

G. Brona, K. Bunkowski, A. Byszuk³⁶, K. Doroba, A. Kalinowski, M. Konecki, J. Krolikowski, M. Misiura, M. Olszewski, M. Walczak

Laboratório de Instrumentação e Física Experimental de Partículas, Lisboa, Portugal

P. Bargassa, C. Beirão Da Cruz E Silva, A. Di Francesco, P. Faccioli, P.G. Ferreira Parracho,

M. Gallinaro, J. Hollar, N. Leonardo, L. Lloret Iglesias, F. Nguyen, J. Rodrigues Antunes, J. Seixas, O. Toldaiev, D. Vadruccio, J. Varela, P. Vischia

Joint Institute for Nuclear Research, Dubna, Russia

S. Afanasiev, P. Bunin, M. Gavrilenco, I. Golutvin, I. Gorbunov, A. Kamenev, V. Karjavin, A. Lanev, A. Malakhov, V. Matveev^{37,38}, P. Moisenz, V. Palichik, V. Perelygin, S. Shmatov, S. Shulha, N. Skatchkov, V. Smirnov, A. Zarubin

Petersburg Nuclear Physics Institute, Gatchina (St. Petersburg), Russia

V. Golovtsov, Y. Ivanov, V. Kim³⁹, E. Kuznetsova, P. Levchenko, V. Murzin, V. Oreshkin, I. Smirnov, V. Sulimov, L. Uvarov, S. Vavilov, A. Vorobyev

Institute for Nuclear Research, Moscow, Russia

Yu. Andreev, A. Dermenev, S. Gninenko, N. Golubev, A. Karneyeu, M. Kirsanov, N. Krasnikov, A. Pashenkov, D. Tlisov, A. Toropin

Institute for Theoretical and Experimental Physics, Moscow, Russia

V. Epshteyn, V. Gavrilov, N. Lychkovskaya, V. Popov, I. Pozdnyakov, G. Safronov, A. Spiridonov, E. Vlasov, A. Zhokin

National Research Nuclear University 'Moscow Engineering Physics Institute' (MEPhI), Moscow, Russia

A. Bylinkin

P.N. Lebedev Physical Institute, Moscow, Russia

V. Andreev, M. Azarkin³⁸, I. Dremin³⁸, M. Kirakosyan, A. Leonidov³⁸, G. Mesyats, S.V. Rusakov

Skobeltsyn Institute of Nuclear Physics, Lomonosov Moscow State University, Moscow, Russia

A. Baskakov, A. Belyaev, E. Boos, A. Demiyanov, A. Ershov, A. Gribushin, O. Kodolova, V. Korotkikh, I. Loktin, I. Myagkov, S. Obraztsov, S. Petrushanko, V. Savrin, A. Snigirev, I. Vardanyan

State Research Center of Russian Federation, Institute for High Energy Physics, Protvino, Russia

I. Azhgirey, I. Bayshev, S. Bitioukov, V. Kachanov, A. Kalinin, D. Konstantinov, V. Krychkine, V. Petrov, R. Ryutin, A. Sobol, L. Tourtchanovitch, S. Troshin, N. Tyurin, A. Uzunian, A. Volkov

University of Belgrade, Faculty of Physics and Vinca Institute of Nuclear Sciences, Belgrade, Serbia

P. Adzic⁴⁰, P. Cirkovic, J. Milosevic, V. Rekovic

Centro de Investigaciones Energéticas Medioambientales y Tecnológicas (CIEMAT), Madrid, Spain

J. Alcaraz Maestre, E. Calvo, M. Cerrada, M. Chamizo Llatas, N. Colino, B. De La Cruz, A. Delgado Peris, A. Escalante Del Valle, C. Fernandez Bedoya, J.P. Fernández Ramos, J. Flix, M.C. Fouz, P. Garcia-Abia, O. Gonzalez Lopez, S. Goy Lopez, J.M. Hernandez, M.I. Josa, E. Navarro De Martino, A. Pérez-Calero Yzquierdo, J. Puerta Pelayo, A. Quintario Olmeda, I. Redondo, L. Romero, J. Santaolalla, M.S. Soares

Universidad Autónoma de Madrid, Madrid, Spain

C. Albajar, J.F. de Trocóniz, M. Missiroli, D. Moran

Universidad de Oviedo, Oviedo, Spain

J. Cuevas, J. Fernandez Menendez, S. Folgueras, I. Gonzalez Caballero, E. Palencia Cortezon, J.M. Vizan Garcia

Instituto de Física de Cantabria (IFCA), CSIC-Universidad de Cantabria, Santander, Spain

I.J. Cabrillo, A. Calderon, J.R. Castiñeiras De Saa, P. De Castro Manzano, M. Fernandez, J. Garcia-Ferrero, G. Gomez, A. Lopez Virto, J. Marco, R. Marco, C. Martinez Rivero, F. Matorras, J. Piedra Gomez, T. Rodrigo, A.Y. Rodriguez-Marrero, A. Ruiz-Jimeno, L. Scodellaro, N. Trevisani, I. Vila, R. Vilar Cortabitarte

CERN, European Organization for Nuclear Research, Geneva, Switzerland

D. Abbaneo, E. Auffray, G. Auzinger, M. Bachtis, P. Baillon, A.H. Ball, D. Barney, A. Benaglia, J. Bendavid, L. Benhabib, G.M. Berruti, P. Bloch, A. Bocci, A. Bonato, C. Botta, H. Breuker, T. Camporesi, R. Castello, G. Cerminara, M. D'Alfonso, D. d'Enterria, A. Dabrowski, V. Daponte, A. David, M. De Gruttola, F. De Guio, A. De Roeck, S. De Visscher, E. Di Marco⁴¹, M. Dobson, M. Dordevic, B. Dorney, T. du Pree, D. Duggan, M. Dünser, N. Dupont, A. Elliott-Peisert, G. Franzoni, J. Fulcher, W. Funk, D. Gigi, K. Gill, D. Giordano, M. Girone, F. Glege, R. Guida, S. Gundacker, M. Guthoff, J. Hammer, P. Harris, J. Hegeman, V. Innocente, P. Janot, H. Kirschenmann, M.J. Kortelainen, K. Kousouris, K. Krajczar, P. Lecoq, C. Lourenço, M.T. Lucchini, N. Magini, L. Malgeri, M. Mannelli, A. Martelli, L. Masetti, F. Meijers, S. Mersi, E. Meschi, F. Moortgat, S. Morovic, M. Mulders, M.V. Nemallapudi, H. Neugebauer, S. Orfanelli⁴², L. Orsini, L. Pape, E. Perez, M. Peruzzi, A. Petrilli, G. Petrucciani, A. Pfeiffer, M. Pierini, D. Piparo, A. Racz, T. Reis, G. Rolandi⁴³, M. Rovere, M. Ruan, H. Sakulin, C. Schäfer, C. Schwick, M. Seidel, A. Sharma, P. Silva, M. Simon, P. Sphicas⁴⁴, J. Steggemann, B. Stieger, M. Stoye, Y. Takahashi, D. Treille, A. Triossi, A. Tsirou, G.I. Veres²¹, N. Wardle, H.K. Wöhri, A. Zagozdzinska³⁶, W.D. Zeuner

Paul Scherrer Institut, Villigen, Switzerland

W. Bertl, K. Deiters, W. Erdmann, R. Horisberger, Q. Ingram, H.C. Kaestli, D. Kotlinski, U. Langenegger, D. Renker, T. Rohe

Institute for Particle Physics, ETH Zurich, Zurich, Switzerland

F. Bachmair, L. Bäni, L. Bianchini, B. Casal, G. Dissertori, M. Dittmar, M. Donegà, P. Eller, C. Grab, C. Heidegger, D. Hits, J. Hoss, G. Kasieczka, P. Lecomte[†], W. Lustermann, B. Mangano, M. Marionneau, P. Martinez Ruiz del Arbol, M. Masciovecchio, D. Meister, F. Micheli, P. Musella, F. Nessi-Tedaldi, F. Pandolfi, J. Pata, F. Pauss, L. Perrozzi, M. Quitnat, M. Rossini, M. Schönenberger, A. Starodumov⁴⁵, M. Takahashi, V.R. Tavolaro, K. Theofilatos, R. Wallny

Universität Zürich, Zurich, Switzerland

T.K. Arrestad, C. Amsler⁴⁶, L. Caminada, M.F. Canelli, V. Chiochia, A. De Cosa, C. Galloni, A. Hinzmann, T. Hreus, B. Kilminster, C. Lange, J. Ngadiuba, D. Pinna, G. Rauco, P. Robmann, F.J. Ronga, D. Salerno, Y. Yang

National Central University, Chung-Li, Taiwan

M. Cardaci, K.H. Chen, T.H. Doan, Sh. Jain, R. Khurana, M. Konyushikhin, C.M. Kuo, W. Lin, Y.J. Lu, A. Pozdnyakov, S.S. Yu

National Taiwan University (NTU), Taipei, Taiwan

Arun Kumar, P. Chang, Y.H. Chang, Y.W. Chang, Y. Chao, K.F. Chen, P.H. Chen, C. Dietz, F. Fiori, U. Grundler, W.-S. Hou, Y. Hsiung, Y.F. Liu, R.-S. Lu, M. Miñano Moya, E. Petrakou, J.f. Tsai, Y.M. Tzeng

Chulalongkorn University, Faculty of Science, Department of Physics, Bangkok, Thailand
B. Asavapibhop, K. Kovitanggoon, G. Singh, N. Srimanobhas, N. Suwonjandee

Cukurova University, Adana, Turkey

A. Adiguzel, M.N. Bakirci⁴⁷, S. Cerci⁴⁸, Z.S. Demiroglu, C. Dozen, I. Dumanoglu, E. Eskut, F.H. Gecit, S. Girgis, G. Gokbulut, Y. Guler, E. Gurpinar, I. Hos, E.E. Kangal⁴⁹, G. Onengut⁵⁰, M. Ozcan, K. Ozdemir⁵¹, A. Polatoz, D. Sunar Cerci⁴⁸, C. Zorbilmez

Middle East Technical University, Physics Department, Ankara, Turkey

B. Bilin, S. Bilmis, B. Isildak⁵², G. Karapinar⁵³, M. Yalvac, M. Zeyrek

Bogazici University, Istanbul, Turkey

E. Glmez, M. Kaya⁵⁴, O. Kaya⁵⁵, E.A. Yetkin⁵⁶, T. Yetkin⁵⁷

Istanbul Technical University, Istanbul, Turkey

A. Cakir, K. Cankocak, S. Sen⁵⁸, F.I. Vardarli

Institute for Scintillation Materials of National Academy of Science of Ukraine, Kharkov, Ukraine

B. Grynyov

National Scientific Center, Kharkov Institute of Physics and Technology, Kharkov, Ukraine

L. Levchuk, P. Sorokin

University of Bristol, Bristol, United Kingdom

R. Aggleton, F. Ball, L. Beck, J.J. Brooke, E. Clement, D. Cussans, H. Flacher, J. Goldstein, M. Grimes, G.P. Heath, H.F. Heath, J. Jacob, L. Kreczko, C. Lucas, Z. Meng, D.M. Newbold⁵⁹, S. Paramesvaran, A. Poll, T. Sakuma, S. Seif El Nasr-storey, S. Senkin, D. Smith, V.J. Smith

Rutherford Appleton Laboratory, Didcot, United Kingdom

A. Belyaev⁶⁰, C. Brew, R.M. Brown, L. Calligaris, D. Cieri, D.J.A. Cockerill, J.A. Coughlan, K. Harder, S. Harper, E. Olaiya, D. Petyt, C.H. Shepherd-Themistocleous, A. Thea, I.R. Tomalin, T. Williams, S.D. Worm

Imperial College, London, United Kingdom

M. Baber, R. Bainbridge, O. Buchmuller, A. Bundock, D. Burton, S. Casasso, M. Citron, D. Colling, L. Corpe, P. Dauncey, G. Davies, A. De Wit, M. Della Negra, P. Dunne, A. Elwood, D. Futyan, G. Hall, G. Iles, R. Lane, R. Lucas⁵⁹, L. Lyons, A.-M. Magnan, S. Malik, J. Nash, A. Nikitenko⁴⁵, J. Pela, M. Pesaresi, K. Petridis, D.M. Raymond, A. Richards, A. Rose, C. Seez, A. Tapper, K. Uchida, M. Vazquez Acosta⁶¹, T. Virdee, S.C. Zenz

Brunel University, Uxbridge, United Kingdom

J.E. Cole, P.R. Hobson, A. Khan, P. Kyberd, D. Leslie, I.D. Reid, P. Symonds, L. Teodorescu, M. Turner

Baylor University, Waco, USA

A. Borzou, K. Call, J. Dittmann, K. Hatakeyama, H. Liu, N. Pastika

The University of Alabama, Tuscaloosa, USA

O. Charaf, S.I. Cooper, C. Henderson, P. Rumerio

Boston University, Boston, USA

D. Arcaro, A. Avetisyan, T. Bose, D. Gastler, D. Rankin, C. Richardson, J. Rohlf, L. Sulak, D. Zou

Brown University, Providence, USA

J. Alimena, E. Berry, D. Cutts, A. Ferapontov, A. Garabedian, J. Hakala, U. Heintz, E. Laird, G. Landsberg, Z. Mao, M. Narain, S. Piperov, S. Sagir, R. Syarif

University of California, Davis, Davis, USA

R. Breedon, G. Breto, M. Calderon De La Barca Sanchez, S. Chauhan, M. Chertok, J. Conway, R. Conway, P.T. Cox, R. Erbacher, G. Funk, M. Gardner, W. Ko, R. Lander, C. Mclean, M. Mulhearn, D. Pellett, J. Pilot, F. Ricci-Tam, S. Shalhout, J. Smith, M. Squires, D. Stolp, M. Tripathi, S. Wilbur, R. Yohay

University of California, Los Angeles, USA

R. Cousins, P. Everaerts, A. Florent, J. Hauser, M. Ignatenko, D. Saltzberg, E. Takasugi, V. Valuev, M. Weber

University of California, Riverside, Riverside, USA

K. Burt, R. Clare, J. Ellison, J.W. Gary, G. Hanson, J. Heilman, M. Ivova PANEVA, P. Jandir, E. Kennedy, F. Lacroix, O.R. Long, M. Malberti, M. Olmedo Negrete, A. Shrinivas, H. Wei, S. Wimpenny, B. R. Yates

University of California, San Diego, La Jolla, USA

J.G. Branson, G.B. Cerati, S. Cittolin, R.T. D'Agnolo, M. Derdzinski, A. Holzner, R. Kelley, D. Klein, J. Letts, I. Macneill, D. Olivito, S. Padhi, M. Pieri, M. Sani, V. Sharma, S. Simon, M. Tadel, A. Vartak, S. Wasserbaech⁶², C. Welke, F. Würthwein, A. Yagil, G. Zevi Della Porta

University of California, Santa Barbara, Santa Barbara, USA

J. Bradmiller-Feld, C. Campagnari, A. Dishaw, V. Dutta, K. Flowers, M. Franco Sevilla, P. Geffert, C. George, F. Golf, L. Gouskos, J. Gran, J. Incandela, N. Mccoll, S.D. Mullin, J. Richman, D. Stuart, I. Suarez, C. West, J. Yoo

California Institute of Technology, Pasadena, USA

D. Anderson, A. Apresyan, A. Bornheim, J. Bunn, Y. Chen, J. Duarte, A. Mott, H.B. Newman, C. Pena, M. Spiropulu, J.R. Vlimant, S. Xie, R.Y. Zhu

Carnegie Mellon University, Pittsburgh, USA

M.B. Andrews, V. Azzolini, A. Calamba, B. Carlson, T. Ferguson, M. Paulini, J. Russ, M. Sun, H. Vogel, I. Vorobiev

University of Colorado Boulder, Boulder, USA

J.P. Cumalat, W.T. Ford, A. Gaz, F. Jensen, A. Johnson, M. Krohn, T. Mulholland, U. Nauenberg, K. Stenson, S.R. Wagner

Cornell University, Ithaca, USA

J. Alexander, A. Chatterjee, J. Chaves, J. Chu, S. Dittmer, N. Eggert, N. Mirman, G. Nicolas Kaufman, J.R. Patterson, A. Rinkevicius, A. Ryd, L. Skinnari, L. Soffi, W. Sun, S.M. Tan, W.D. Teo, J. Thom, J. Thompson, J. Tucker, Y. Weng, P. Wittich

Fermi National Accelerator Laboratory, Batavia, USA

S. Abdullin, M. Albrow, G. Apollinari, S. Banerjee, L.A.T. Bauerick, A. Beretvas, J. Berryhill, P.C. Bhat, G. Bolla, K. Burkett, J.N. Butler, H.W.K. Cheung, F. Chlebana, S. Cihangir, V.D. Elvira, I. Fisk, J. Freeman, E. Gottschalk, L. Gray, D. Green, S. Grünendahl, O. Gutsche, J. Hanlon, D. Hare, R.M. Harris, S. Hasegawa, J. Hirschauer, Z. Hu, B. Jayatilaka, S. Jindariani, M. Johnson, U. Joshi, B. Klima, B. Kreis, S. Lammel, J. Linacre, D. Lincoln, R. Lipton, T. Liu, R. Lopes De Sá, J. Lykken, K. Maeshima, J.M. Marraffino, S. Maruyama, D. Mason, P. McBride, P. Merkel, S. Mrenna, S. Nahm, C. Newman-Holmes[†], V. O'Dell, K. Pedro, O. Prokofyev, G. Rakness,

E. Sexton-Kennedy, A. Soha, W.J. Spalding, L. Spiegel, S. Stoynev, N. Strobbe, L. Taylor, S. Tkaczyk, N.V. Tran, L. Uplegger, E.W. Vaandering, C. Vernieri, M. Verzocchi, R. Vidal, M. Wang, H.A. Weber, A. Whitbeck

University of Florida, Gainesville, USA

D. Acosta, P. Avery, P. Bortignon, D. Bourilkov, A. Carnes, M. Carver, D. Curry, S. Das, R.D. Field, I.K. Furic, S.V. Gleyzer, J. Konigsberg, A. Korytov, K. Kotov, P. Ma, K. Matchev, H. Mei, P. Milenovic⁶³, G. Mitselmakher, D. Rank, R. Rossin, L. Shchutska, M. Snowball, D. Sperka, N. Terentyev, L. Thomas, J. Wang, S. Wang, J. Yelton

Florida International University, Miami, USA

S. Hewamanage, S. Linn, P. Markowitz, G. Martinez, J.L. Rodriguez

Florida State University, Tallahassee, USA

A. Ackert, J.R. Adams, T. Adams, A. Askew, S. Bein, J. Bochenek, B. Diamond, J. Haas, S. Hagopian, V. Hagopian, K.F. Johnson, A. Khatiwada, H. Prosper, M. Weinberg

Florida Institute of Technology, Melbourne, USA

M.M. Baarmann, V. Bhopatkar, S. Colafranceschi⁶⁴, M. Hohlmann, H. Kalakhety, D. Noonan, T. Roy, F. Yumiceva

University of Illinois at Chicago (UIC), Chicago, USA

M.R. Adams, L. Apanasevich, D. Berry, R.R. Betts, I. Bucinskaite, R. Cavanaugh, O. Evdokimov, L. Gauthier, C.E. Gerber, D.J. Hofman, P. Kurt, C. O'Brien, I.D. Sandoval Gonzalez, H. Trauger, P. Turner, N. Varelas, Z. Wu, M. Zakaria

The University of Iowa, Iowa City, USA

B. Bilki⁶⁵, W. Clarida, K. Dilsiz, S. Durgut, R.P. Gundrajula, M. Haytmyradov, V. Khristenko, J.-P. Merlo, H. Mermerkaya⁶⁶, A. Mestvirishvili, A. Moeller, J. Nachtman, H. Ogul, Y. Onel, F. Ozok⁶⁷, A. Penzo, C. Snyder, E. Tiras, J. Wetzel, K. Yi

Johns Hopkins University, Baltimore, USA

I. Anderson, B.A. Barnett, B. Blumenfeld, N. Eminizer, D. Fehling, L. Feng, A.V. Gritsan, P. Maksimovic, C. Martin, M. Osherson, J. Roskes, A. Sady, U. Sarica, M. Swartz, M. Xiao, Y. Xin, C. You

The University of Kansas, Lawrence, USA

P. Baringer, A. Bean, G. Benelli, C. Bruner, R.P. Kenny III, D. Majumder, M. Malek, M. Murray, S. Sanders, R. Stringer, Q. Wang

Kansas State University, Manhattan, USA

A. Ivanov, K. Kaadze, S. Khalil, M. Makouski, Y. Maravin, A. Mohammadi, L.K. Saini, N. Skhirtladze, S. Toda

Lawrence Livermore National Laboratory, Livermore, USA

D. Lange, F. Rebassoo, D. Wright

University of Maryland, College Park, USA

C. Anelli, A. Baden, O. Baron, A. Belloni, B. Calvert, S.C. Eno, C. Ferraioli, J.A. Gomez, N.J. Hadley, S. Jabeen, R.G. Kellogg, T. Kolberg, J. Kunkle, Y. Lu, A.C. Mignerey, Y.H. Shin, A. Skuja, M.B. Tonjes, S.C. Tonwar

Massachusetts Institute of Technology, Cambridge, USA

A. Apyan, R. Barbieri, A. Baty, K. Bierwagen, S. Brandt, W. Busza, I.A. Cali, Z. Demiragli, L. Di Matteo, G. Gomez Ceballos, M. Goncharov, D. Gulhan, Y. Iiyama, G.M. Innocenti, M. Klute,

D. Kovalskyi, Y.S. Lai, Y.-J. Lee, A. Levin, P.D. Luckey, A.C. Marini, C. McGinn, C. Mironov, S. Narayanan, X. Niu, C. Paus, C. Roland, G. Roland, J. Salfeld-Nebgen, G.S.F. Stephans, K. Sumorok, M. Varma, D. Velicanu, J. Veverka, J. Wang, T.W. Wang, B. Wyslouch, M. Yang, V. Zhukova

University of Minnesota, Minneapolis, USA

B. Dahmes, A. Evans, A. Finkel, A. Gude, P. Hansen, S. Kalafut, S.C. Kao, K. Klapoetke, Y. Kubota, Z. Lesko, J. Mans, S. Nourbakhsh, N. Ruckstuhl, R. Rusack, N. Tambe, J. Turkewitz

University of Mississippi, Oxford, USA

J.G. Acosta, S. Oliveros

University of Nebraska-Lincoln, Lincoln, USA

E. Avdeeva, R. Bartek, K. Bloom, S. Bose, D.R. Claes, A. Dominguez, C. Fangmeier, R. Gonzalez Suarez, R. Kamaliuddin, D. Knowlton, I. Kravchenko, F. Meier, J. Monroy, F. Ratnikov, J.E. Siado, G.R. Snow

State University of New York at Buffalo, Buffalo, USA

M. Alyari, J. Dolen, J. George, A. Godshalk, C. Harrington, I. Iashvili, J. Kaisen, A. Kharchilava, A. Kumar, S. Rappoccio, B. Roozbahani

Northeastern University, Boston, USA

G. Alverson, E. Barberis, D. Baumgartel, M. Chasco, A. Hortiangtham, A. Massironi, D.M. Morse, D. Nash, T. Orimoto, R. Teixeira De Lima, D. Trocino, R.-J. Wang, D. Wood, J. Zhang

Northwestern University, Evanston, USA

S. Bhattacharya, K.A. Hahn, A. Kubik, J.F. Low, N. Mucia, N. Odell, B. Pollack, M. Schmitt, K. Sung, M. Trovato, M. Velasco

University of Notre Dame, Notre Dame, USA

A. Brinkerhoff, N. Dev, M. Hildreth, C. Jessop, D.J. Karmgard, N. Kellams, K. Lannon, N. Marinelli, F. Meng, C. Mueller, Y. Musienko³⁷, M. Planer, A. Reinsvold, R. Ruchti, G. Smith, S. Taroni, N. Valls, M. Wayne, M. Wolf, A. Woodard

The Ohio State University, Columbus, USA

L. Antonelli, J. Brinson, B. Bylsma, L.S. Durkin, S. Flowers, A. Hart, C. Hill, R. Hughes, W. Ji, T.Y. Ling, B. Liu, W. Luo, D. Puigh, M. Rodenburg, B.L. Winer, H.W. Wulsin

Princeton University, Princeton, USA

O. Driga, P. Elmer, J. Hardenbrook, P. Hebda, S.A. Koay, P. Lujan, D. Marlow, T. Medvedeva, M. Mooney, J. Olsen, C. Palmer, P. Piroué, D. Stickland, C. Tully, A. Zuranski

University of Puerto Rico, Mayaguez, USA

S. Malik

Purdue University, West Lafayette, USA

A. Barker, V.E. Barnes, D. Benedetti, D. Bortolotto, L. Gutay, M.K. Jha, M. Jones, A.W. Jung, K. Jung, A. Kumar, D.H. Miller, N. Neumeister, B.C. Radburn-Smith, X. Shi, I. Shipsey, D. Silvers, J. Sun, A. Svyatkovskiy, F. Wang, W. Xie, L. Xu

Purdue University Calumet, Hammond, USA

N. Parashar, J. Stupak

Rice University, Houston, USA

A. Adair, B. Akgun, Z. Chen, K.M. Ecklund, F.J.M. Geurts, M. Guilbaud, W. Li, B. Michlin, M. Northup, B.P. Padley, R. Redjimi, J. Roberts, J. Rorie, Z. Tu, J. Zabel

University of Rochester, Rochester, USA

B. Betchart, A. Bodek, P. de Barbaro, R. Demina, Y. Eshaq, T. Ferbel, M. Galanti, A. Garcia-Bellido, J. Han, A. Harel, O. Hindrichs, A. Khukhunaishvili, K.H. Lo, G. Petrillo, P. Tan, M. Verzetti

Rutgers, The State University of New Jersey, Piscataway, USA

J.P. Chou, E. Contreras-Campana, D. Ferencek, Y. Gershtein, E. Halkiadakis, D. Hidas, E. Hughes, S. Kaplan, R. Kunawalkam Elayavalli, A. Lath, K. Nash, H. Saka, S. Salur, S. Schnetzer, D. Sheffield, S. Somalwar, R. Stone, S. Thomas, P. Thomassen, M. Walker

University of Tennessee, Knoxville, USA

M. Foerster, G. Riley, K. Rose, S. Spanier

Texas A&M University, College Station, USA

O. Bouhali⁶⁸, A. Castaneda Hernandez⁶⁸, A. Celik, M. Dalchenko, M. De Mattia, A. Delgado, S. Dildick, R. Eusebi, J. Gilmore, T. Huang, T. Kamon⁶⁹, V. Krutelyov, R. Mueller, I. Osipenkov, Y. Pakhotin, R. Patel, A. Perloff, A. Rose, A. Safonov, A. Tatarinov, K.A. Ulmer²

Texas Tech University, Lubbock, USA

N. Akchurin, C. Cowden, J. Damgov, C. Dragoiu, P.R. Dudero, J. Faulkner, S. Kunori, K. Lamichhane, S.W. Lee, T. Libeiro, S. Undleeb, I. Volobouev

Vanderbilt University, Nashville, USA

E. Appelt, A.G. Delannoy, S. Greene, A. Gurrola, R. Janjam, W. Johns, C. Maguire, Y. Mao, A. Melo, H. Ni, P. Sheldon, S. Tuo, J. Velkovska, Q. Xu

University of Virginia, Charlottesville, USA

M.W. Arenton, B. Cox, B. Francis, J. Goodell, R. Hirosky, A. Ledovskoy, H. Li, C. Lin, C. Neu, T. Sinthuprasith, X. Sun, Y. Wang, E. Wolfe, J. Wood, F. Xia

Wayne State University, Detroit, USA

C. Clarke, R. Harr, P.E. Karchin, C. Kottachchi Kankamamge Don, P. Lamichhane, J. Sturdy

University of Wisconsin - Madison, Madison, WI, USA

D.A. Belknap, D. Carlsmith, M. Cepeda, S. Dasu, L. Dodd, S. Duric, B. Gomber, M. Grothe, R. Hall-Wilton, M. Herndon, A. Hervé, P. Klabbers, A. Lanaro, A. Levine, K. Long, R. Loveless, A. Mohapatra, I. Ojalvo, T. Perry, G.A. Pierro, G. Polese, T. Ruggles, T. Sarangi, A. Savin, A. Sharma, N. Smith, W.H. Smith, D. Taylor, P. Verwilligen, N. Woods

†: Deceased

1: Also at Vienna University of Technology, Vienna, Austria

2: Also at CERN, European Organization for Nuclear Research, Geneva, Switzerland

3: Also at State Key Laboratory of Nuclear Physics and Technology, Peking University, Beijing, China

4: Also at Institut Pluridisciplinaire Hubert Curien, Université de Strasbourg, Université de Haute Alsace Mulhouse, CNRS/IN2P3, Strasbourg, France

5: Also at National Institute of Chemical Physics and Biophysics, Tallinn, Estonia

6: Also at Skobeltsyn Institute of Nuclear Physics, Lomonosov Moscow State University, Moscow, Russia

7: Also at Universidade Estadual de Campinas, Campinas, Brazil

-
- 8: Also at Centre National de la Recherche Scientifique (CNRS) - IN2P3, Paris, France
 - 9: Also at Laboratoire Leprince-Ringuet, Ecole Polytechnique, IN2P3-CNRS, Palaiseau, France
 - 10: Also at Joint Institute for Nuclear Research, Dubna, Russia
 - 11: Also at Helwan University, Cairo, Egypt
 - 12: Now at Zewail City of Science and Technology, Zewail, Egypt
 - 13: Also at British University in Egypt, Cairo, Egypt
 - 14: Now at Ain Shams University, Cairo, Egypt
 - 15: Also at Université de Haute Alsace, Mulhouse, France
 - 16: Also at Tbilisi State University, Tbilisi, Georgia
 - 17: Also at RWTH Aachen University, III. Physikalisches Institut A, Aachen, Germany
 - 18: Also at University of Hamburg, Hamburg, Germany
 - 19: Also at Brandenburg University of Technology, Cottbus, Germany
 - 20: Also at Institute of Nuclear Research ATOMKI, Debrecen, Hungary
 - 21: Also at Eötvös Loránd University, Budapest, Hungary
 - 22: Also at University of Debrecen, Debrecen, Hungary
 - 23: Also at Wigner Research Centre for Physics, Budapest, Hungary
 - 24: Also at Indian Institute of Science Education and Research, Bhopal, India
 - 25: Also at University of Visva-Bharati, Santiniketan, India
 - 26: Now at King Abdulaziz University, Jeddah, Saudi Arabia
 - 27: Also at University of Ruhuna, Matara, Sri Lanka
 - 28: Also at Isfahan University of Technology, Isfahan, Iran
 - 29: Also at University of Tehran, Department of Engineering Science, Tehran, Iran
 - 30: Also at Plasma Physics Research Center, Science and Research Branch, Islamic Azad University, Tehran, Iran
 - 31: Also at Università degli Studi di Siena, Siena, Italy
 - 32: Also at Purdue University, West Lafayette, USA
 - 33: Also at International Islamic University of Malaysia, Kuala Lumpur, Malaysia
 - 34: Also at Malaysian Nuclear Agency, MOSTI, Kajang, Malaysia
 - 35: Also at Consejo Nacional de Ciencia y Tecnología, Mexico city, Mexico
 - 36: Also at Warsaw University of Technology, Institute of Electronic Systems, Warsaw, Poland
 - 37: Also at Institute for Nuclear Research, Moscow, Russia
 - 38: Now at National Research Nuclear University 'Moscow Engineering Physics Institute' (MEPhI), Moscow, Russia
 - 39: Also at St. Petersburg State Polytechnical University, St. Petersburg, Russia
 - 40: Also at Faculty of Physics, University of Belgrade, Belgrade, Serbia
 - 41: Also at INFN Sezione di Roma; Università di Roma, Roma, Italy
 - 42: Also at National Technical University of Athens, Athens, Greece
 - 43: Also at Scuola Normale e Sezione dell'INFN, Pisa, Italy
 - 44: Also at National and Kapodistrian University of Athens, Athens, Greece
 - 45: Also at Institute for Theoretical and Experimental Physics, Moscow, Russia
 - 46: Also at Albert Einstein Center for Fundamental Physics, Bern, Switzerland
 - 47: Also at Gaziosmanpasa University, Tokat, Turkey
 - 48: Also at Adiyaman University, Adiyaman, Turkey
 - 49: Also at Mersin University, Mersin, Turkey
 - 50: Also at Cag University, Mersin, Turkey
 - 51: Also at Piri Reis University, Istanbul, Turkey
 - 52: Also at Ozyegin University, Istanbul, Turkey
 - 53: Also at Izmir Institute of Technology, Izmir, Turkey
 - 54: Also at Marmara University, Istanbul, Turkey

- 55: Also at Kafkas University, Kars, Turkey
- 56: Also at Istanbul Bilgi University, Istanbul, Turkey
- 57: Also at Yildiz Technical University, Istanbul, Turkey
- 58: Also at Hacettepe University, Ankara, Turkey
- 59: Also at Rutherford Appleton Laboratory, Didcot, United Kingdom
- 60: Also at School of Physics and Astronomy, University of Southampton, Southampton, United Kingdom
- 61: Also at Instituto de Astrofísica de Canarias, La Laguna, Spain
- 62: Also at Utah Valley University, Orem, USA
- 63: Also at University of Belgrade, Faculty of Physics and Vinca Institute of Nuclear Sciences, Belgrade, Serbia
- 64: Also at Facoltà Ingegneria, Università di Roma, Roma, Italy
- 65: Also at Argonne National Laboratory, Argonne, USA
- 66: Also at Erzincan University, Erzincan, Turkey
- 67: Also at Mimar Sinan University, Istanbul, Istanbul, Turkey
- 68: Also at Texas A&M University at Qatar, Doha, Qatar
- 69: Also at Kyungpook National University, Daegu, Korea